A Computational Workbench Environment for Virtual Power Plant Simulation

Quarterly Progress Report

Reporting Period Start Date: January 1, 2003
Reporting Period End Date: March 31, 2003

Mike Bockelie, REI
Dave Swensen, REI
Martin Denison, REI
Connie Senior, REI
Zumao Chen, REI
Temi Linjewile, REI
Adel Sarofim, REI
Bene Risio, RECOM

April 25, 2003

DOE Cooperative Agreement No: DE-FC26-00NT41047

Reaction Engineering International
77 West 200 South, Suite 210
Salt Lake City, UT 84101

Disclaimer

Abstract

This is the tenth Quarterly Technical Report for DOE Cooperative Agreement No: DE-FC26-00NT41047. The goal of the project is to develop and demonstrate a computational workbench for simulating the performance of Vision 21 Power Plant Systems.

Within the last quarter, good progress has been made on all aspects of the project. Calculations for a full Vision 21 plant configuration have been performed for two gasifier types. An improved process model for simulating entrained flow gasifiers has been implemented into the workbench. Model development has focused on: a pre-processor module to compute global gasification parameters from standard fuel properties and intrinsic rate information; a membrane based water gas shift; and reactors to oxidize fuel cell exhaust gas. The data visualization capabilities of the workbench have been extended by implementing the VTK visualization software that supports advanced visualization methods, including inexpensive Virtual Reality techniques. The ease-of-use, functionality and plug-and-play features of the workbench were highlighted through demonstrations of the workbench at a DOE sponsored coal utilization conference. A white paper has been completed that contains recommendations on the use of component architectures, model interface protocols and software frameworks for developing a Vision 21 plant simulator.

Table of Contents

1

Executive Summary

The work to be conducted in this project received funding from the Department of Energy under Cooperative Agreement No: DE-FC26-00NT41047. This project has a period of performance that started on October 1, 2000 and continues through September 30, 2003.

The goal of the project is to develop and demonstrate a computational workbench for simulating the performance of Vision 21 Power Plant Systems. The Year One effort focused on developing a *prototype workbench* for the DOE Low-Emissions Boiler System (LEBS) Proof of Concept (POC) design. The Year Two effort focused on developing a more advanced workbench environment for simulating a gasifier-based Vision 21 energyplex. The Year Three effort has focused on continued development of the workbench environment and application of the workbench to Vision 21 plant configurations.

The main accomplishments during the last three months include:

- Demonstrations of the Vision 21 workbench at an exhibit booth at a DOE sponsored coal utilization conference. Through "live" demonstrations users were shown the ease-of-use, functionality and plug-and-play features of the workbench.

- A "white paper" that describes the findings and recommendations from this project on the use of component architectures, model interface protocols and software frameworks for developing a Vision 21 plant simulator. A complete copy of the white paper is included in the Appendix section of this report. The recommendations include:

    1. **Near term**: Vision 21 simulator frameworks should **support** both **COM** and **CORBA** component architecture versions of the **CAPE_Open** interface standard.

    2. **Long term**: an **improved component model interface should be developed** and deployed to support specific needs of the Vision 21 simulator.

    3. **Frameworks:** We recommend **continued development of Vision 21 simulator framework(s)** that can support the hierarchy of models anticipated for future Vision 21 plant simulations. In the near term, commercially available frameworks will continue to play an important role in Vision 21 simulation. However, it is unclear that there is sufficient motivation for commercially available frameworks to invest the funds needed to extend their simulation tools to have the flexibility and extensibility desired for advanced plant simulation.

- Calculations for a full Vision 21 plant configuration for a two stage, slurry feed entrained flow gasifier modified to have improved cold gas efficiency and for a single stage, dry feed entrained flow gasifier.

- Implemented into the workbench an improved process model for simulating one and two stage entrained flow gasifiers.

- Transient, CFD simulations for the start-up of a gasifier have been performed using a standalone unsteady, gasifier CFD modeling tool executing on a supercomputer.

- Model development efforts for:
  - a pre-processor module to compute global fuel (coal) gasification parameters from standard fuel properties and intrinsic rate information;
  - a membrane based water gas shift reactor to simulate converting CO and H2O to H2 and CO2. This reactor will allow investigating configurations to support greater H2 production and/or CO2 capture; and
  - reactors to oxidize unburned fuel in the exhaust gas of a fuel cell.

- Modified the workbench to use the VTK data visualization software, a package that supports advanced visualization methods, including inexpensive Virtual Reality techniques.

Each of these topics is discussed in the following sections.

3

Experimental Methods

Within this section we present brief discussions on the many sub-tasks that must be addressed in developing the workbench. For simplicity, the discussion items are presented in the order of the Tasks as outlined in our detailed Work Plan.

Task 1 – Program Management

A poster that highlighted material developed within this project was presented at the Society of Industrial and Applied Mathematicians (SIAM) Computational Sciences and Engineering Conference 2003 held in San Diego, California, February 10-14, 2003. The poster, entitled "Computational Simulation Environments" [Swensen et al, 2003a] provided details of the software design and infrastructure used within our Vision 21 workbench.

On Friday, March 6, 2003 project team members held a conference telephone call with Neville Holt (EPRI), a consultant to this project. The meeting provided us the opportunity to discuss our progress on developing entrained flow gasifiers models and potential follow-on applications of the gasifier models developed within this project.

A podium presentation that highlighted material from this project was made at the 28th International Technical Conference on Coal Utilization & Fuel Systems (the Clearwater Conference), held March 10-13, 2003 in Clearwater, Florida, USA [Bockelie et al, 2003b]. The paper, entitled "A Process Workbench for Virtual Simulation of Vision 21 Energyplex Systems" included descriptions of the functionality of the workbench, models contained in the workbench and recent modeling results.

At the Clearwater Conference, REI had a conference booth in which were displayed two posters that highlighted modeling techniques developed within this project. In addition, the booth contained a PC on which "live" demonstrations of our Vision 21 workbench tool were conducted for conference attendees. The booth proved quite successful in providing us the opportunity to demonstrate first hand to personnel from industry, academia and the DOE the capabilities and functionality of our Vision 21 workbench.

- The first poster, entitled "Computational Workbench Environment for Virtual Power Plant Simulation", highlighted the software tools, design and functionality of the workbench system [Bockelie et al, 2003c].
- The second poster, entitled "Model Interchangeability via Component Architectures for Vision 21 Simulation Environments", highlighted our approach for interfacing models within the workbench environment [Swensen et al, 2003b].
- Through use of a PC in the conference booth, conference attendees were shown the basics of using the workbench, including constructing and connecting components, changing model parameters, executing model networks and viewing model outputs. In addition, attendees were able to sit at the computer terminal and use stereographic LCD glasses to view results from the detailed CFD gasifier model using Virtual Reality. The

conference booth was staffed by personnel from Reaction Engineering International and the Iowa State University Virtual Reality Applications Center.

An abstract for a paper entitled "Using Models To Evaluate Gasifier Performance" has been accepted for presentation at the the 20th Annual International Pittsburgh Coal Conference to be held September 15-19, 2003 in Pittsburgh, Pennsylvania, USA [Bockelie et al, 2003d]. The paper will highlight the use of our entrained flow gasifier models.

Our project team has been invited to provide a podium presentation at the upcoming Black Liquor Combustion and Gasification Workshop, to be held May 13-16, 2003 in Park City, Utah. The presentation will highlight the flowing slag model that has been developed and implemented into our entrained flow coal gasifier CFD model [Denison et al, 2003].

Task 2 – Virtual Plant Workbench II

The objective of this task is to further develop the capabilities of the computational workbench environment with the goal of providing the infrastructure needed to model a Vision 21 energyplex system. For the many sub-tasks contained under Task 2, the work effort is being performed by software engineers from Reaction Engineering International (REI) and Visual Influence (VI).

Task 2.1 Software Design

The main focus of this sub-task has been to continue to evolve a comprehensive software design, building on the ideas developed for Workbench I. As the complexity and capabilities of Workbench II continue to increase, the software design is evaluated and modified accordingly.

Component Interfaces

During the last performance period, we have continued to focus our efforts on utilizing component architecture methodologies to interface models to the workbench. We persist in believing this is a vital aspect of the software design. This belief is routinely reinforced as we see component architectures continue to gain momentum as the future of computing and software engineering.

Recently, numerous questions have arisen regarding component architectures and standard interfaces and how they should be utilized in current and future Vision21 software development. To address these questions, we have prepared a white paper that provides a detailed description of these issues. Hopefully, the white paper will serve as a useful guide for all parties involved with the Vision21 program.

In the white paper we summarize our findings and recommendations on the issues of component architectures and component interfaces that are relevant to Vision 21 plant engineering and simulation. These concepts relate to advanced software engineering techniques, originally developed for business applications, that have recently been adopted by the scientific computing community. The advent of the Vision 21 program has probably been the first instance of these software techniques being used in simulations for power generation applications. To keep our descriptions brief, we provide summaries, written in “layman terms”, on component architectures (e.g., COM, CORBA, CCA), component interfaces (e.g., CAPE_Open) and software frameworks (e.g., ASPEN, SCIRun). We highlight only the key concepts that are relevant to Vision 21 simulation. As described within the white paper, direct comparisons between items at different levels of the software engineering hierarchy (e.g., CCA .vs. CAPE_Open) are not appropriate.

Our findings are based on research performed within our Vision 21 project, in conjunction with discussions with personnel involved with Vision 21 and with leading researchers in the fields of high performance computing and scientific computing.

Our findings lead to the following recommendations:

4. **Near term**: Vision 21 simulator frameworks should **support** both **COM** and **CORBA** component architecture versions of the **CAPE_Open** interface standard. We anticipate continued, extensive use of "process flow sheet" models within Vision 21 plant simulations and engineering. This component interface will allow use of process models developed for process flow sheet simulations from commercial and research sources.

5. **Long term**: an **improved component model interface should be developed** and deployed to support specific needs of the Vision 21 simulator. In particular, the inherent limitations on data transfer between components imposed by the CAPE_Open interface should be eliminated to allow utilization of more comprehensive modeling techniques. The enhanced component interface could be developed through judicious extensions to the CAPE_Open standard or by creating a new specification targeted for Vision 21.

6. **Frameworks:** We recommend **continued development of Vision 21 simulator framework(s)** that can support the hierarchy of models anticipated for future Vision 21 plant simulations. In the near term, commercially available frameworks (e.g., ASPEN) will continue to play an important role in Vision 21 simulation. However, it is unclear that there is sufficient motivation for commercially available frameworks to invest the funds needed to extend their simulation tools to have the flexibility and extensibility desired for advanced plant simulation.

A copy of the full white paper is included as an Appendix to this report.

Enhancements to the SCIRun Framework – New Model Execution Scheduler

During the last performance period, the core software infrastructure of the workbench was modified to include a custom execution scheduler (the algorithm which determines which models to execute) that can handle more sophisticated module interconnections, including feedback loops.

This scheduler modification was necessary to address the material "loops" in Vision21 reference configurations. The original scheduler worked entirely within a pure dataflow paradigm and thus did not provide sufficient control over the sequence of models to be executed. In a pure dataflow network, data is provided to the upper most models and as these models complete their execution, the resulting data "flows" to downstream models. This scheme of execution makes the use of feedback loops (data from downstream models as inputs to upstream models) or iteration loops (hold execution in a section of a network until a user specified variable converges) very difficult without significant code rewrite.

The new scheduler employs a directed Painter's algorithm to determine status of the network in combination with several graph analysis algorithms to determine execution order. The new scheduler correctly analyzes and schedules the operations to be performed within a network with single, multiple, or even deeply nested loops. In addition, the scheduler is now "aware" of the status of individual network models or entire network sections. This allows much greater user control of network execution, naturally provides for "global" network variables (such as pressure drop through an entire furnace train) and enhanced error handling.

Task 2.2 Visualization

During the last performance period, we have continued in our effort to further extend the visualization capabilities of the workbench by adding Virtual Reality (VR) capabilities. The goal of these efforts will be to enable the user to visualize complex data sets in a myriad of ways on a full range of visualization hardware, from a simple CRT all the way to a multi-walled, immersive environment.

The basis for the enhanced visualization capabilities comes from two open source packages: VTK and vrJuggler. VTK (Visualization Tool Kit) [http://www.vtk.org] is an extensive class library which supports a full range of scientific visualization operations including the creation of graphical entities for color mapped planes, streamlines, isosurfaces etc. vrJuggler [http://www.vrjuggler.org] is a class library with the capability to abstract VR hardware. vrJuggler makes it possible to create visualizations which can be displayed on a range of hardware, from a CRT all the way to a multi-walled, immersive enclosure.

We have currently completed implementation of a VTK-only viewer. This visualization tool provides a drop-in alternative to OpenDX. The tool adds the capability of being able to generate active stereoscopic views for desktop VR. The viewer supports a full range of visualization capabilities including color-mapped planes, isosurfaces, streamlines, particle trajectories and volume rendering. To launch the viewer for the detailed gasifier module, the user simply clicks the "3D" button on the UI as shown in the figure below.

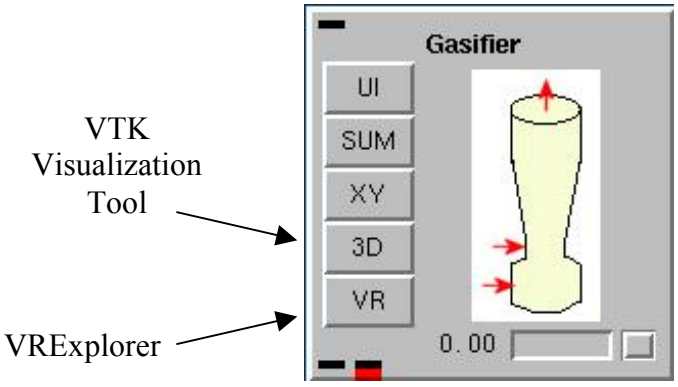

For high-end VR visualization capabilities, we are planning to incorporate the capabilities of Iowa State University's VRAC VRExplorer. Further development of VRExplorer to meet the needs of the workbench will be done through collaborative efforts of both Reaction Engineering International and VRAC center personnel. We believe this collaboration will result in powerful VR capabilities for the workbench, which will be compatible with nearly all VR hardware including that currently being used at NETL.

VRExplorer makes use of both the VTK and vrJuggler class library. Using VTK as only a calculation engine, VRExplorer creates VTK "actor" objects and passes them through

vtkActorToPF [http://brighton.ncsa.uiuc.edu/~prajlich/vtkActorToPF/], which is a small library that converts the information generated by VTK to SGI's OpenGL Performer. Once the information regarding the visualization exists as a Performer scenegraph, VRExplorer is then able to make use of vrJuggler to handle calculations related to hardware abstraction.

Task 2.3 Module Implementation/Integration

The focus of this sub-task is to integrate into the workbench component modules for Vision 21 plant equipment models, as they are developed and ready for use in the workbench.

Component Model Integration:

During the last performance period model integration activities have included keeping the process gasifier model up-to-date and to evaluate potential software modifications required to implement the membrane and fuel cell – gas turbine combustor models that are in development (see description of Task 3.3).

Task 2.4 Vision 21 Workbench Demonstration

During March10-13, 2003, the Vision 21 workbench was demonstrated at the International Technical Conference on Coal Utilization & Fuel Systems in Clearwater, Florida. The conference booth was staffed by personel from Reaction Engineering International and Iowa State Universities VRAC center. Conference attendees were shown the basics of using the workbench, including constructing and connecting components, changing model parameters, executing model networks and viewing model outputs. In addition, attendees were able to sit at the computer terminal, and using stereographic LCD glasses, view results from the detailed gasifier model using Virtual Reality techniques.

Task 3 – Model Vision 21 Components

The purpose of this task is to develop the reactor and CFD models for the components that will be included in the workbench. In general, these models are first developed in a "stand-alone" form and then subsequently integrated into the workbench environment.

Vision 21 Energy Plex Configuration

Illustrated in Figure 1 is the Vision 21 energyplex configuration that the DOE Vision 21 Program Manager has suggested be used by this project to demonstrate the capabilities of our workbench environment. This configuration consists of an entrained flow gasifier, gas clean up system, gas turbines, heat recovery steam generator, steam turbine and SOFC fuel cells. As described below, a combination of CFD and reactor models will be used to simulate the performance of this configuration. A CFD model will be used for the entrained flow gasifier and simpler models will be used for the remainder of the equipment and processes.

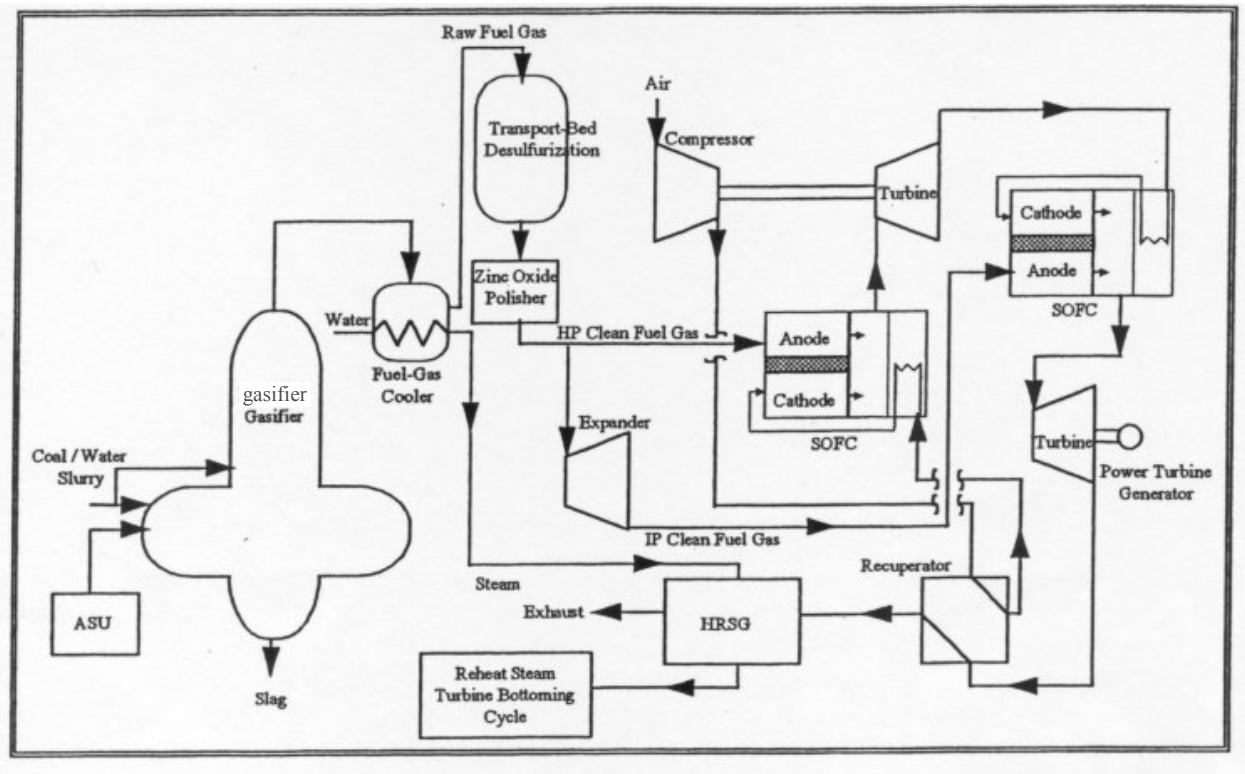

Figure 1. DOE selected Vision 21 test case configuration.

Listed in Tables 1 and 2 are the gross conditions for the configuration that were originally provided by DOE. Shown in Figure 2 is a mass and energy balance sheet obtained from DOE that provides more detailed information about the targeted Vision 21 configuration. A comparison of Figures 1 and 2 shows some discrepancies. As noted in previous progress reports, where information is missing we have used data available in the literature, combined with engineering judgment, to develop the required information to create the needed models.

Table 1. Provided Operating Conditions for Vision 21 Energyplex

Gasifier (18 atm)	Two-stage, up-fired
Coal Input to Gasifier (lb/hr)	256,142
Coal Type	Illinois #6
Thermal Input (MW)	875.8
HP SOFC dc/ac	189.4/182.8
LP SOFC dc/ac	121.4/117.2
Gas Turbine, MW	133.7
Steam Turbine, MW	118.0
Fuel Expander, MW	9.6
Gross Power	561.3
Auxiliary Power, MW	40.4
Net Power, MW	520.9
Efficiency, % HHV	59.5

Table 2. Illinois Coal #6 Description

Proximate Analysis	As-Received (wt%)
Moisture	11.12
Ash	9.70
Volatile Matter	34.99
Fixed Carbon	44.19
TOTAL	100.00
HHV (Btu/lb)	11666
Ultimate Analysis	**As-Received (wt%)**
Moisture	11.12
Carbon	63.75
Hydrogen	4.50
Nitrogen	1.25
Sulfur	0.29
Ash	9.70
Oxygen (by difference)	6.88
TOTAL	100.00

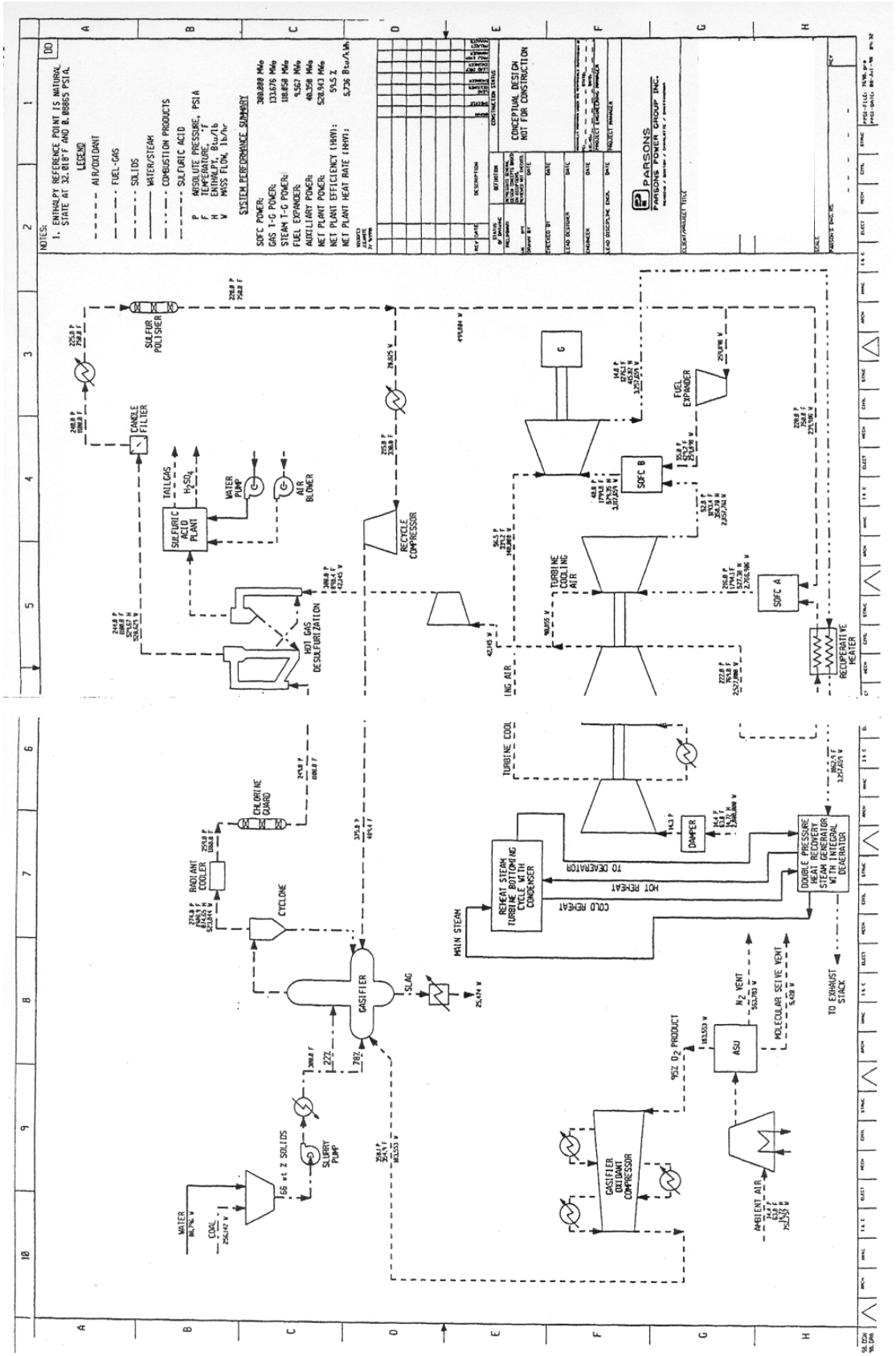

Figure 2. Mass and Energy Balance sheet provided by DOE for Vision 21 reference configuration.

Task 3.3 Gasifier Models

Good progress has been made on developing CFD based models for entrained flow gasifiers. The models are being created using two different CFD codes. REI personnel will develop one gasifier model with *GLACIER* - a comprehensive two-phase CFD based reacting CFD code. At present, *GLACIER* is limited to performing steady-state simulations and thus will be used to perform steady state CFD simulations of single and two-stage gasifiers. The other gasifier model will be developed by RECOM using *AIOLOS*, a comprehensive reacting CFD code capable of performing transient boiler simulations and thus will be used to perform time dependent simulations for a single stage gasifier. Both CFD codes have been used to analyze numerous coal-fired industrial combustion systems. The two codes employ different meshing technologies and different assumptions and sub-models for turbulence-chemistry interaction, simulating two-phase flow and reaction kinetics for combustion and gasification.

Below we highlight the progress within the last performance period in developing the CFD based gasifier models.

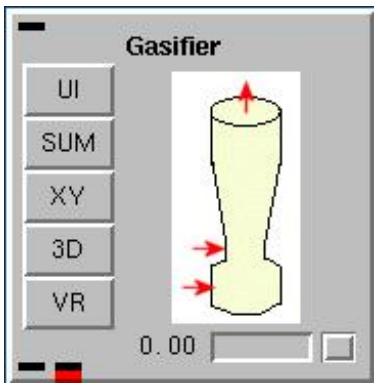

***GLACIER* Gasifier Module (Steady State):**. During the last performance period, our efforts for this model have focused on completion of a 0D pre-processor gasifier model and performing simulations to allow comparing our model results versus previous DOE NETL reported values for Vision 21 conditions. Details about the model development are described immediately below, whereas further details on the CFD and system results are described in the Results and Discussion Section of this report.

0-D Gasifier Model

The CFD gasifier model requires significant computational time to arrive at a steady-state solution. Hence, there is a need for a simpler model that may be used for faster calculations either within the energyplex workbench or as a preprocessor to optimize operating inputs before running the CFD model. The model can be used to optimize gasifier efficiency while providing indicators for proper slag flow. During the last performance period this model was extended to remove the assumption of complete burnout in the first stage when modeling two stage gasifiers.

The 0-D gasifier model consists of two submodels: an zonal equilibrium submodel with heat transfer and a coal burnout submodel. The zonal submodel calculates the equilibrium exit gas concentration and temperature given a prescribed heat transfer through the walls. An ash viscosity submodel from the CFD gasifier slag model is used to calculate a representative ash viscosity and critical viscosity temperature. The fuel burnout and char recycle are required inputs to the zonal submodel obtained from the burnout submodel, while the gas and radiation temperatures are the required inputs into the burnout submodel obtained from the zonal submodel. A schematic of the 0D model for a one and two stage gasifier are illustrated in Figures 3a and 3b, respectively.

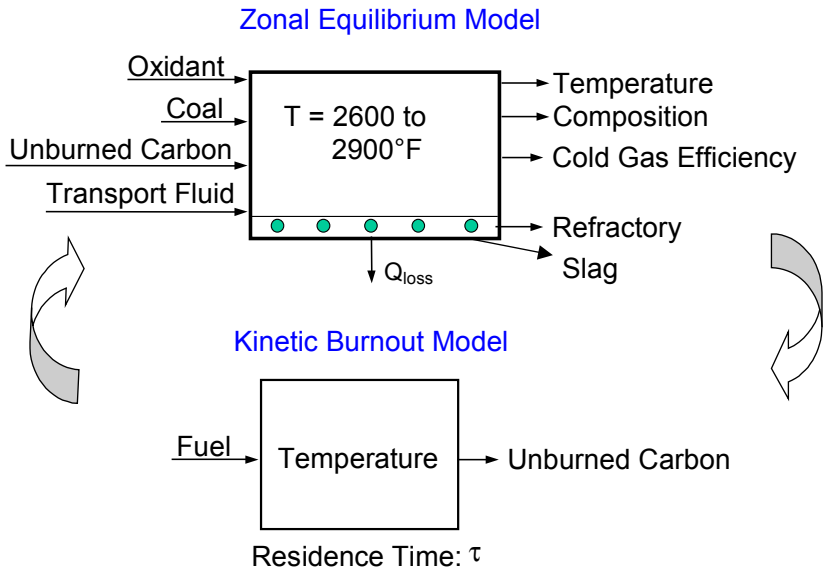

Figure 3a. Schematic for the one stage, 0-D gasifier pre-processor model.

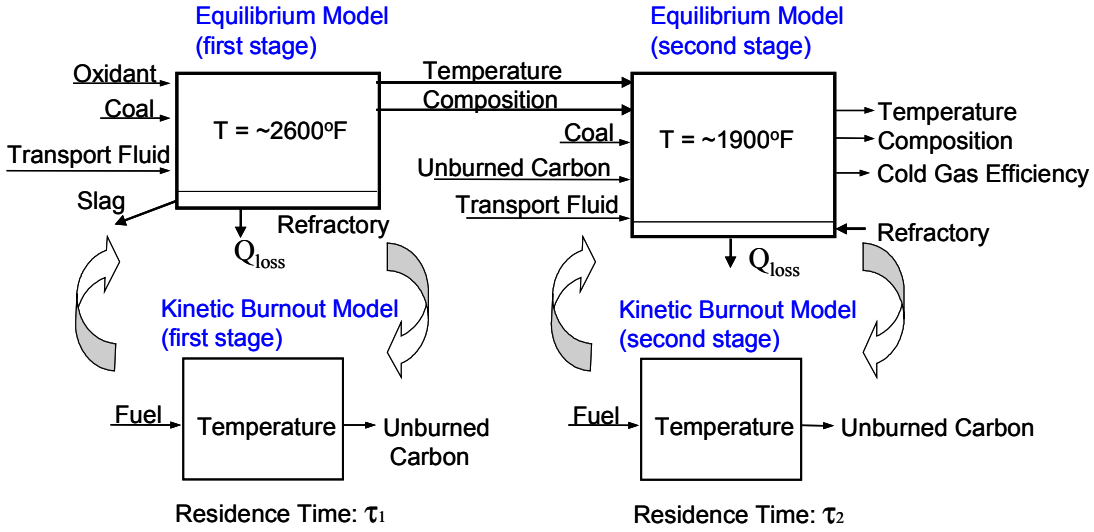

Figure 3b. Schematic for the two-stage, 0-D gasifier model.

For particle burnout we originally used CBK8, a model developed at Brown University [Sun and Hurt, 2000] which includes intrinsic oxidation of coal in lean pulverized combustion. However, CBK8 was not formulated for fuel staging and reducing conditions such as needed to model two stage gasifiers. Hence, during the last performance period we have replaced CBK8 with an in-house heterogeneous particle reaction model. This model is extensible for use with other kinetic data that we anticipate will be become available from the Collaborative Research Center for Coal and Sustainable Development (CCSD) in Australia.

Two-stage gasifiers are operated with the first stage serving as a combustion stage, which provides the heat needed to drive endothermic gasification reactions in the reducing second stage. The first stage is operated closer to stoichiometric, while the remaining feed-stock fuel is introduced in the second stage with very little or no oxidant. During the last performance period, we have completed the extension of the 0D gasifier model for two stage gasifiers to allow burnout be calculated in the first stage. Previously, complete burnout in the first stage was assumed. With the new particle burnout model (see above), staged fuel injection is easily handled. Iterations proceed in the first stage between the particle burnout, equilibrium, and heat transfer models until the exit temperature is converged (see Figure 3b). The same iterations for the second stage then follow, except that any unburned particles from the first stage are also integrated in the second stage.

Intrinsic Kinetics Pre-Processor

The purpose of this sub-task is to develop a module (*PREKIN*) to generate global gasification rate parameters that are compatible with the REI gasifier models from standard fuel (coal) properties and intrinsic kinetics data. The PREKIN module is summarized in Figure 4.

Inputs for PREKIN will include the:

- Conversion level (default: 90%) at which global rate will be optimized.
- Temperature range at which global rate will be optimized: T and ΔT (default: T and ± 20%)
- Mean particle size and standard deviation
- Pressure (default 1 atmosphere)
- Fuel properties: C, H, Ash, and ASTM volatile (default PRB, Illinois 6)
- Intrinsic kinetic parameters: pre-exponential factor, activation energy, and reaction order

As noted in Figure 4, the global rate parameters to be calculated by *PREKIN* include the

- A_G, pre-exponential factor (kgC/m^2-s-Pa^m),
- E_G, apparent activation energy (J/kmol), and
- m, apparent reaction order

from the following Arrhenius-type expression for the gasification rate, q_{rxn} (kgC/m^2-s):

$$q_{rxn} = A_G \cdot \exp\left(-\frac{E_G}{R \cdot T_P}\right) \cdot (P_s)^m$$

where R is gas constant (8314.51 J/kmol-K), T particle temperature (K), P_s reactant partial pressure (Pa). The global rate parameters will be calculated by (1) computing gasification rates at various reaction conditions (i.e., determined by the conversion level at varying O_2 concentration and temperature) and then (2) applying an optimization routine to fit the reacting rates. In the

optimization routine, the reaction parameters will be fit with equation (B) in Figure 4 by either changing all three parameters (m, E_G, and A_G) or by changing two parameters (m and A_G) at a fixed E_G (7.325E+07 J/kmol-K).

Inputs:
- Fuel properties: C, H, O, Ash, and Volatile matter
- Particle size distribution
- Intrinsic rate parameters in equation (A):
  - Reaction order (n)
  - Activation energy (E)
  - Pre-exponential factor (k_o)
- Reaction Conditions: temperature, pressure

PREKIN

Kinetic pre-processor
- Generate gasification rate based on input temperature and pressure
- Combination of various sub-models:
  - Devolatilization
  - Porosity development
  - Thermal annealing
  - Ash inhibition
  - Diffusion
  - CO/CO_2
  - Gasification rate
- Fitting and Optimization the results with the equation (B)

$$q_{prekin} = \eta \cdot k_o \cdot \exp\left(-\frac{E}{R \cdot T_P}\right) \cdot \left(\frac{P_s}{R \cdot T_P}\right)^n \cdot s \cdot \sigma_A \cdot \gamma \qquad \text{(A)}$$

$$q_{rxn} = A_G \cdot \exp\left(-\frac{E_G}{R \cdot T_P}\right) \cdot (P_s)^m \qquad \text{(B)}$$

Outputs:
- Global rate parameters:
  - pre-exponential factor (A_G)
  - activation energy (E_G)
  - apparent reaction order (m) in equation (B)

Figure 4. *PREKIN* Kinetic pre-processor.

PREKIN will include the following sub-models for the processes that occur for gasification of a solid fuel:

- Devolatilization
- Porosity development
- Thermal annealing
- Ash inhibition
- Reactant diffusion
- CO/CO_2 ratio at the char surface
- Gasification rate based on intrinsic rate expression

The specific sub-models from the literature to be used in *PREKIN* are listed in Table 3.

The pre-processor will be developed with a phased approach using a modular software design that will allow for sub-model modification and enhancement. The initial version of the tool will be created by modifying sub-models currently in-use by REI. Data from the open literature will be used to compare the predicted and reported kinetic values over a range of conditions. Based on these comparisons, we anticipate replacing key sub-models with more advanced sub-models. In particular, we anticipate:

a) devolatilization: replace existing model with combination of CPD model [Fletcher et al, 1992] and Kobayashi's two step model [Kobayshi et al, 1976];
b) char porosity: replace Power law model [Smith, 1971] with char pore topology model [Gavalas, 1981].
c) CO/CO2 at char surface: replace current relation with SKIPPY (Surface Kinetics In Porous Particles) model, developed by Haynes [Muris and Haynes, 1999], that calculates species concentration profiles for the reaction of a porous solid in a reacting gaseous environment at pseudo-steady state.

The proposed approach of developing the model in stages will allow developing a more mechanistic based understanding, and model, of the processes that impact gasification kinetics.

At completion, *PREKIN* will provide the capability to generate proper gasification rate parameters, by coal type, that can be directly used in REI's gasification model.

..

Table 3. Initial and Final sub-models for *PREKIN*

Process	Initial Model	Final Model
Devolatilization	High temperature volatile yield is required, if not provided, the code consider 120% of ASTM volatile as high temperature volatiles	Chemical Percolation Devolatilization (CPD) model and/or Kobayashi's two step model for volatile yield
Porosity development	Power law by Smith	Gavalas or other Model including evolution of pore size distribution for different regimes of combustion
Thermal annealing	Distributed activation energy annealing model	Evaluate with NSC model to show negative activation energy regime
Effect of mineral matter (Ash Inhibition)	Two effects are implemented 1) Mass transport: resistance to oxygen transport to the reacting surface 2) Dilution effect: mineral matter can occupy volume within the particle and thus reduce the carbon mass an carbon surface available per unit particle volume. Neglects vaporization and inorganic reaction	--
Reactant diffusion	Constant Sherwood number (2) Constant τ/f in effective diffusivity calculation (τ is tortuosity and f is fraction of the total porosity in feeder pores)	--
CO/CO_2 ratio at the char surface	$CO/CO_2 = A_C \cdot \exp(-E_C/R \cdot T_P)$ where • A_C is 200 and • E_C 3.768E+07 J/kmol-K, • T_p particle temperature, and • R gas constant[5].	Competing mechanism (SKIPPY)
Gasification rate	$q_{prekin} = \eta \cdot k_o \cdot \exp\left(-\frac{E}{R \cdot T_P}\right) \cdot \left(\frac{P_s}{R \cdot T_P}\right)^n \cdot s \cdot \sigma_A \cdot \gamma$ where • q_{PREKIN} (kgC/m^2-s) is the rate of reaction (expressed per unit external area of solid), • γ (cm) the characteristic dimension of the particle (volume/unit external area, d/6), • η is the effectiveness factor, • s (m^2/kgC) the specific surface area, • σ_A (kgC/m^3) the carbon density in the particle, • ko (kgC/s-m^2-(mol/m^3)^n) the intrinsic reactivity coefficient, and • n the true reaction order.	Possible replacement by Langmuir-Hinshelwood for CO_2, H_2O, H_2 gasification

Task 3.4 Combustors

Based on discussions with the DOE, we intend to implement a suite of combustor models within our Vision 21 workbench to allow investigating different technologies for the power block. We will include models to analyze plant configurations based on a hybrid power block with a fuel cell gas turbine (FC-GT) system or a power block based on a direct fired, hydrogen burning gas turbine. The hybrid power block will be based on the Vision 21 configuration in Figures 1-2. The hydrogen fired turbine will be appropriate for plant configurations in which hydrogen production is a major objective, such as in the recently announced DOE *Futuregen* initiative.

Each system presents a different challenge. In a hybrid configuration, the fuel cell only achieves about 85% fuel conversion. Hence, there is a low temperature, low heating value (Low-BTU) exhaust gas stream from the fuel cell that must be processed (oxidized) before sending the exhaust gas to downstream equipment. Due to the low heating value of the gas, this exhaust stream can be quite difficult to oxidize (i.e., avoiding flame blowout). Here, we intend to develop two models. One will be a "dump" combustor based on designs from the open literature for processing "off-gas" or "waste gas" streams. The second model will be for a catalytic combustor. Here, we will again draw upon information in the open literature. For the hydrogen fired gas turbine, probably the greatest challenge is providing adequate cooling or tempering of the flame within the combustor. The proposed combustor configuration will be based on information in the open literature.

Use of the models within the workbench will allow identification of operating parameters that influence efficiency such as fuel gas inlet temperature, residence time, gas velocity, adiabatic combustion temperature and fuel/air ratio. Obtaining both full fuel conversion and minimal pollutant emissions will be important.

To summarize, in this sub-task we intend to develop and implement into the workbench models for a:

- "dump" combustor to oxidize Low-BTU exhaust gas from a fuel cell
- catalytic combustor to oxidize Low-BTU exhaust gas from a fuel cell
- combustor for a hydrogen fired gas turbine.

All designs will be based on information in the open literature and engineering judgment.

In the following we provide further technical details on the models and summarize their current development status.

Dump Combustor

Over the past quarter, development has begun on a dump combustor model that will be included in the Vision 21 workbench. The dump combustor would be placed downstream of the solid oxide fuel cells. Fuel cells typically have about 85% fuel utilization. The remaining, un-reacted fuel contains available energy that must be extracted in order to obtain high overall plant efficiency. However, the un-reacted fuel cell exhaust is also dilute and the energy density is low. The low energy density requires special combustors. Possibilities for combusting the lean gas include catalytic combustion and dump combustors. To date, only preliminary research has been done on the requirements of a dump combustor for the specific fuel gas under consideration. In the following, we describe kinetic simulations that have been performed for predicted fuel cell exhaust (FCX) gas, along with estimation of required combustor size, and a preliminary modeling approach.

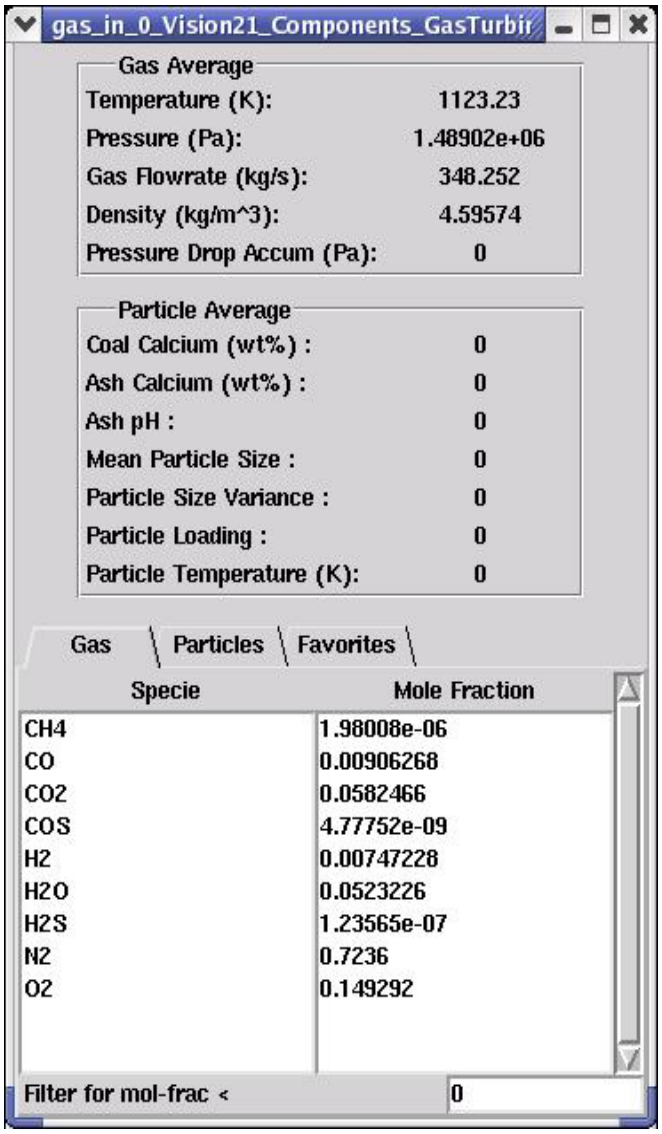

Figure 5. High pressure SOFC exhaust.

The Vision 21 flow diagram of Figure 2 includes high and low pressure Solid Oxide Fuel Cells (SOFC) operating at 14.7 and 3.3 atm, respectively. Figure 5 gives the properties of this gas for the high pressure FCX gas; the low pressure FCX gas is similar. Important characteristics of this gas are the temperature, pressure, energy density, and oxidizer content. Combustion stability and rate is of primary concern in a dump combustor for the gas considered. Combustion rates generally increase with increasing pressure. Also note that the oxygen content is very high in the gas, the stoichiometric ratio for the high pressure gas is 18. Thus, no air needs to be added to the gas. This results in an energy density of 4.8 Btu/scfm. In contrast, typical Molten Carbonate Fuel Cell (MCFC) exhaust contains 30-40 Btu/scfm (S.R. = 1) (Gemmen, 1998), and for comparison, methane contains about 80 Btu/scfm (S.R. = 1). Because the gas is so dilute, the adiabatic equilibrium temperature is only 120 K higher than the inlet gas, so high combustion temperatures will not be achieved. Note the relatively high temperature of the gas, 850 ^{o}C. Currently, a SOFC operates at a high temperature (~900 ^{o}C). At these high temperatures, pressures and oxygen concentration, combustion is very fast, and (with good mixing) could occur in the ductwork exiting a fuel cell.

Figure 6 shows detailed kinetic simulations of the high pressure gas at two inlet temperatures, for a plug flow reactor. The curve shows fuel conversion (CO + H2) versus residence time. These calculations were performed using the GRImech 3.0 kinetic mechanism (G.P. Smith et. al.). As shown in the figure, at the high (typical) combustion temperature given in Figure 5, complete fuel conversion is achieved in about 0.1 seconds residence time. Long term, the goal for SOFC development is to reduce the operating temperature to the range of 550 – 800 ^{o}C (823-1073 K). The 700 K curve shows the effect of the reduced gas temperature on the fuel conversion. Only 90% conversion is achieved at 0.5 seconds, and 97% conversion at 1 second. At lower temperatures catalytic combustion may be required.

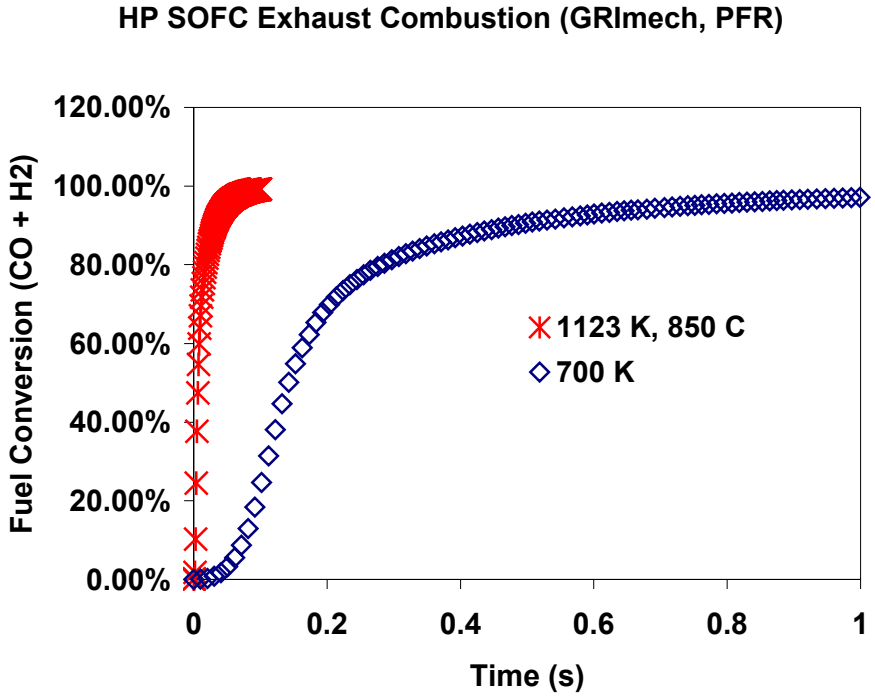

Figure 6. PFR kinetic simulation of high pressure fuel cell exhaust gas.

Preliminary estimation of combustor size is based on an experimental combustor for MCFC exhaust gases (Gemmen, 1998). The experimental configuration was scaled up by assuming geometric similarity (equal length/diameter), and is based on an 0.5 second gas residence time, and the proportionality of reactor volume to temperature, flow rate, and inverse pressure. The combustor dimensions for the high pressure FCX gas conditions of Figure 5 would be 1.5 meters in diameter, and 18 meters long.

The expected model approach is to simulate the combustor as a Bragg combustor, consisting of a perfectly stirred reactor (PSR), followed by a plug flow reactor (PFR). The PSR simulates the flame (or injection) zone, and the PFR simulates the burnout region. Because of the high excess oxygen in the fuel gas stream, no air staging would be needed. The unit would be sized based on a typical length-to-diameter ratio, and an acceptable gas velocity. A user interface similar to other modules will be developed.

Catalytic Combustor

In fuel cell applications, catalytic combustion offers an efficient means of recovering heat from the low heating value fuel cell effluent streams that may otherwise be difficult to burn directly. This is particularly manifest in molten carbonate fuel cell (MCFC) systems where the cell discharges unreacted fuel at about 600°C. In these systems, the anode exhaust containing the unreacted fuel is mixed with air and then oxidized completely in a catalytic combustor (Ghezel-Ayagh and Maru, 2002). At present, solid oxide fuel cell (SOFC) systems operate at temperatures in the window of 800 – 1000°C, because the oxygen ion conduction in yttria stabilized zirconia (YSZ) is best in this temperature window. However, with the current push for low temperature solid electrolytes for SOFC systems, the operating temperature window is likely to fall in the range 700 – 800°C where catalytic oxidation of the lean fuel/air mixtures is an attractive option. In addition to the ability to burn lean fuel/air mixtures completely (Tucci, 1982), catalytic combustors operate at low enough temperatures such that NO_x emissions are minimized (Kolaczkowski, 1995).

Key issues in realizing the potentials of catalytic combustion for hybrid FC/GT systems are:

- Identification of operating parameters that influence efficiency such as gas inlet temperature, residence time, gas velocity, adiabatic combustion temperature and fuel/air ratio.
- Avoiding very high flow rates that lead to blowout.
- Extension of catalyst life by controlling operating conditions.

A review of the literature (Bond et al., 1996; Chou et al., 2000) reveals that the majority of existing models are limited to modeling heterogeneous reactions within a single channel of a monolith for combustion of methane. Although such models are important in interpretation of experimental data, their usefulness for overall design and development is limited.

REI will build upon our modeling expertise for SCR catalysts for NO_x reduction. A single-channel approach will be followed for catalytic oxidation of H_2 and CO. The coupling of heterogeneous reactions and gas phase reactions, fluid flow and heat transfer will be modeled to provide useful data about conditions within the channels. The geometry of the catalyst monolith to be modeled will be based on current catalytic combustors used in FC/GT hybrid applications. The processes in a single monolith channel are shown in Figure 7.

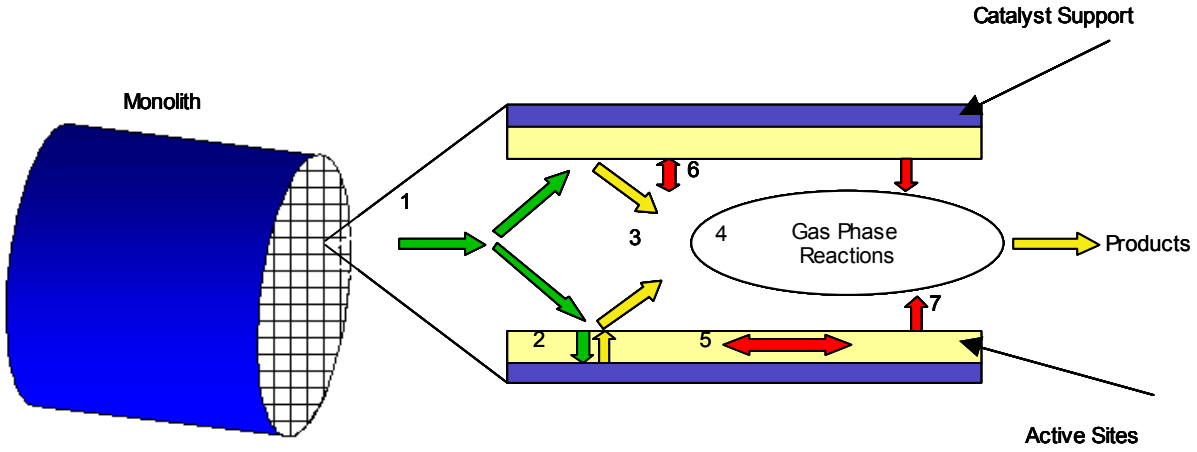

Figure 7. Processes in a single monolith channel. (1) Fuel and air flow into the channel, (2) Diffusion and surface reaction, (3) Desorption of products, (4) Gas phase reactions, (5) Conduction, (6) Radiation, and (7) Convection.

Applications of the model will include:

- Identification of operating parameters that influence efficiency such as inlet temperature, gas velocity, combustion temperature, fuel/air ratio and pressure.
- Identification of flow rates that lead to blowout conditions (extinguishing of reaction).
- Prediction of light-off conditions (initiation of catalytic combustion).
- Tool for guiding the development of concepts, design, scale-up and operation strategies of hybrid FC/GT systems.

Task 3.6 Gas Cleanup and other equipment models

In this sub-task we will develop many of the modules required to simulate the Vision 21 energyplex system. This will include models for the:

- Syngas Cooler
- Heat Recovery Steam Generator
- Gas Recuperator
- SCR
- Turbines, compressors and expanders
- Cyclone separator
- Gas Clean Up
- Water Gas Shift
- High and Low Pressure Solid Oxide Fuel Cell

These systems are modeled with 0D, or at most 1D, reactor models. Except for the Water Gas Shift reactor, all of the remaining models have been described in previous quarterly reports and publications [Bockelie et al, 2003b].

In the following we describe our progress on developing a model for a Water Gas Shift reactor.

Water Gas Shift Membrane Reactor

A membrane reactor model has been developed to simulate the conversion of the syngas product of coal gasification to hydrogen fuel via the water gas shift reaction (WGS):

$$CO + H_2O = CO_2 + H_2 \qquad \text{Eq. 1}$$

The importance of this reaction lies in the ability to convert CO (along with steam) to H_2, which is valuable both as a fuel and as a chemical feedstock. In addition, as CO_2 sequestration becomes more important, the use of H_2 as a clean-burning fuel for fuel cell or combustion power generation is attractive. The water gas shift reaction converts CO, to CO_2, which can be separated from hydrogen and subsequently sequestered.

A membrane reactor for WGS is a two-zone catalytic, fixed-bed, reactor with an integrated hydrogen selective membrane. Syngas enters and reacts on the feed-side of the membrane, and hydrogen permeates to and is carried away by a sweep gas on the permeate side of the membrane. By selectively removing the hydrogen product, high reaction conversions are possible. A membrane reactor module would be positioned after gas cleanup units and before fuel cells, combustors, or other equipment which would process the hydrogen product gas. A completed standalone version of the model has been developed and tested as described below. Integration of the model into the Vision 21 workbench and development of the user interface will be done during the next performance period.

Reaction Characteristics

The WGS reaction occurs at high temperatures, is exothermic (ΔH_{rxn} = -41 J/mole), and equilibrium limited. Thus conversion of CO to H_2 is favored at low temperatures. In order to

achieve sufficient reaction rates at lower temperatures, however, the reaction is carried over a catalyst. Because the reaction is exothermic, the temperature rises with conversion. Conventional WGS reactors operate in two stages with intercooling in between. The first stage operates over a (typically) promoted ferrochrome catalyst at a higher temperature of between 600-750 K, where the bulk of the reaction occurs. The second stage operates at lower temperature with a CuZn-based catalyst (Ma and Lund, 2003), allowing higher H_2 yields.

Figure 8 shows the WGS equilibrium CO conversion as a function of temperature for several feed compositions. These curves give the theoretical maximum conversion of CO to hydrogen in a conventional reactor (without membrane separation), for various initial compositions. The stoichiometric curve is with equimolar amounts of CO and H_2O in the feed and no other species initially. The H_2O:CO = 2 curve is the stoichiometric curve with twice the initial steam, again no products initially. As shown in the figure, higher conversions are possible at a given temperature when running excess steam. This is explained by the WGS equilibrium constant given by

$$K(T) = \frac{[H_2] \cdot [CO_2]}{[CO] \cdot [H_2O]}, \qquad \text{Eq. 2}$$

where [species] denotes the gas concentration of a species. Because the moles of product equal the moles of reactant, the concentration of each species can be replaced with mole fraction of each species, or moles of each species in the gas. As expected, at a given temperature (fixed K) the equilibrium curve shifts to higher CO conversion (H_2 production) when the initial steam is increased, to maintain the equilibrium constant given by Eq. 2. Steam is often injected in order to increase equilibrium conversion, mitigate carbon deposition, and control temperature increases. If product species are present initially, the CO conversion decreases relative to the reactant-only condition. The syngas curve in Figure 8 is the CO conversion with a typical gasifier exhaust taken from a gasifier simulation, as given in Table 4. The maximum CO conversion is so low because the H_2O:CO ratio is less than one—H_2O acts as a limiting reagent. When steam is injected into this gas to give an H_2O:CO ratio of one the maximum conversion increases, but the conversion is generally less than the stoichiometric reactants-only curve because WGS products are present initially. Inert species have no effect on the WGS equilibrium, although reaction rates would be adversely affected by large amounts of inert or diluent species.

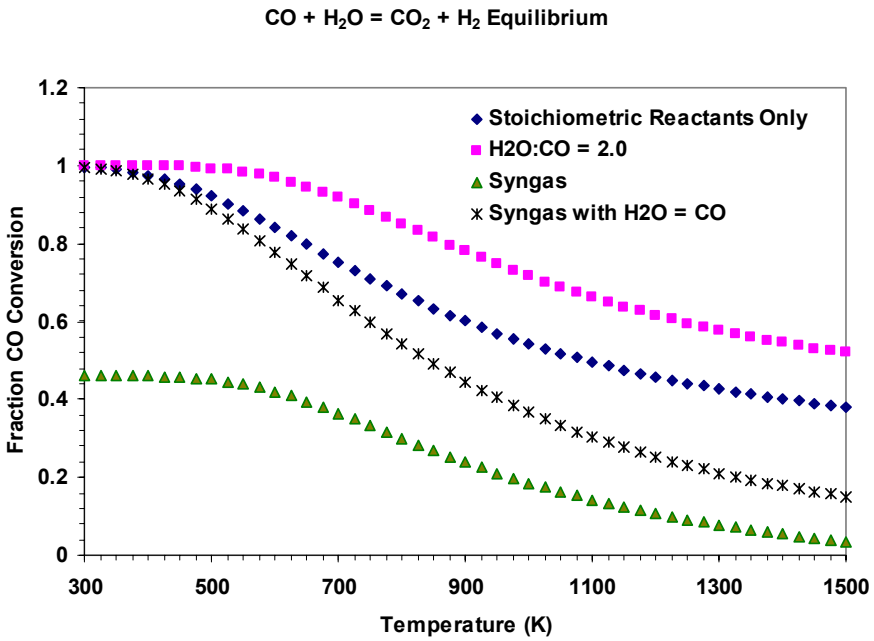

Figure 8. Water gas shift equilibrium conversion for several initial compositions.

Table 4. Gasifier product composition.

Species	Simulated Gasifier Product (Cleaned)
AR	0.87%
CO	42.83%
CO_2	8.34%
H_2	27.42%
H_2O	19.70%
N_2	0.84%

In order to overcome the equilibrium constraints outlined above, an attractive alternative to conventional WGS reactors is to combine a catalytic reactor with a hydrogen selective membrane. The membrane simultaneously allows purification of the hydrogen product, and shifts the WGS reaction toward higher equilibrium conversion by continually removing hydrogen product from the gas stream. The equilibrium constraint is not removed, rather, the equilibrium conversion can be made complete. In addition, the operating temperature requirements are no longer dictated by chemical conversion, but only by material constraints such as catalyst operating temperature, membrane requirements, etc.

Membrane Reactor Configuration

For large-scale applications, parallel banks of concentric tubular arrangements are considered the best option to combine large membrane areas with construction requirements (Bracht, et. al., 1997). Figure 9 shows a schematic of a typical configuration in which catalyst pellets fill the reaction/feed side of the membrane, with a sweep/H2 product gas flowing on the permeate-side

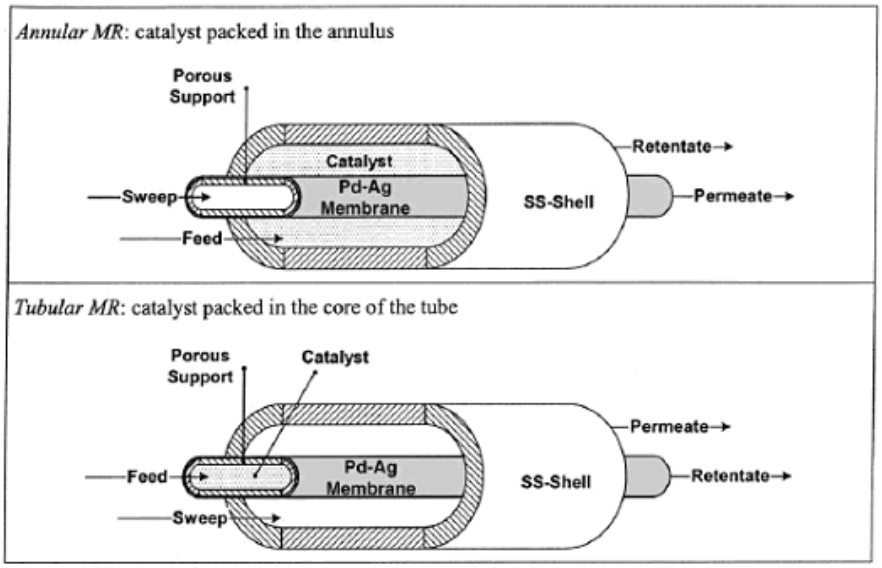

G. Marigliano et al. / Catalysis Today 67 (2001) 85–99

Figure 9. Catalytic membrane reactor configurations.

of the membrane reactor. The figure shows two possible arrangements with the reaction occurring either in the annulus or in the circular pipe. The upper configuration seems to be more popular than that with reaction occurring in the inner tube, and this configuration is assumed in the model (Bracht et. al., 1997), (Devarajan et. al., 1991). Marigliano et. al. (2001) found that the annular feed configuration gave higher conversions for the same reactor size.

Membrane Properties

The membrane of choice for hydrogen removal is a thin metal palladium, or palladium alloy on a porous support. The porous support is required to provide mechanical strength given a relatively large pressure difference across the membrane. Other membrane materials consist of microporous ceramic membranes in which Knudsen diffusion occurs. These membranes are not as selective to hydrogen since the diffusion rate is inversely proportional to the square root of the species molecular weight. Palladium is 100% selective to hydrogen; the hydrogen being transported by a solution-diffusion mechanism. Solution diffusion is governed by a square root pressure driving force due to dissociation of H_2 to H atoms in the metal (Devarajan et. al. 1991). The thickness of the palladium film is on the order of 10 microns. This thin layer is required to allow high hydrogen permeation, which is inversely proportional to the membrane thickness. The hydrogen permeation rate is given by

$$N_P = \frac{P_o \cdot \exp(-E_p / R \cdot T)}{l} \cdot (\sqrt{P_{H2}{}^R} - \sqrt{P_{H2}{}^P}), \qquad \text{Eq. 3}$$

where P_o is a prexponential factor, E_p is the permeation activation energy, l is the membrane thickness and P_{H2} is the hydrogen partial pressure, and Np is the hydrogen flux (moles/m_2 * s).

Palladium membranes are subject to deactivation by sulfur species, so it is important that the gas be cleaned prior to introduction into the membrane. Damle et. al. say that palladium is stable in reducing hydrogen environment with H_2S levels < 100 ppm, which are much higher than levels exiting a warm gas cleanup zinc oxide sulfur polisher expected for Vision 21 gas cleaning. Edlund (1994) says that operational lifetimes greater than 2 years are expected with projected membrane module costs of \$275/ft^2. Pure palladium metal tend to become embrittled by hydrogen, thus a palladium alloy is typically employed.

Model Description

The following is a description of the membrane reactor (MR) model for Vision 21. The model currently exists in a stand-alone form and is not yet fully integrated into the Vision 21 workbench. The MR is a one dimensional model that integrates the hydrogen flux across the catalyst over the length of the unit. The MR is divided into two zones, the feed or reaction zone and the product or permeation zone. Each zone is assumed to be in plug flow, with no axial dispersion. A sweep gas (typically nitrogen and/or steam) is required to reduce the hydrogen product partial pressure. The feed and sweep gases flow concurrently with the feed gas flowing in the annulus and the permeate flowing in the inner tube.

The MR is assumed to be adiabatic with no heat transfer across the membrane between the two zones. A heat loss term from the reaction side to the environment is allowed however, and is specified as a fraction of the inlet gas sensible heat relative to 298 K. This heat loss is assumed uniform over the length of the reactor and is treated as a sink term in the energy equation to be solved.

The hydrogen permeation rate is assumed to be the limiting process; chemical reactions are assumed fast compared to hydrogen permeation. Thus, the feed gas is assumed to be in chemical equilibrium, and all catalytic reaction dependencies are ignored. This assumption has been used and validated in models in the literature (Damle et. al. 1994), (Devarajan et. al. 1991). Only chemical equilibrium for the water gas shift reaction is assumed, all other species are assumed inert. This option simplifies the solution procedure and, more importantly, allows reasonable computation times. Full equilibrium among 23 species was tested, with totally unrealistic results, as expected at relatively low temperatures of 700 K. However, as catalysts are designed to increase reaction rates and be selective to the desired reaction, equilibrium limited to the WGS reaction is reasonable.

To allow further flexibility, the model is configured with an option to simulate the requirements of a staged operation in which the feed gas is first introduced to a pre-shift catalytic non-membrane reactor, cooled and then fed to the membrane reactor. A schematic of this option is presented in Figure 10, taken from Bracht et. al. (1997). As equilibrium is assumed with the aid

of a catalyst, the pre-shift reactor is simply modeled as an adiabatic equilibrium on the feed gas. The temperature of the gas is then dropped to a user-specified value as injected into the MR, with the required heat duty computed.

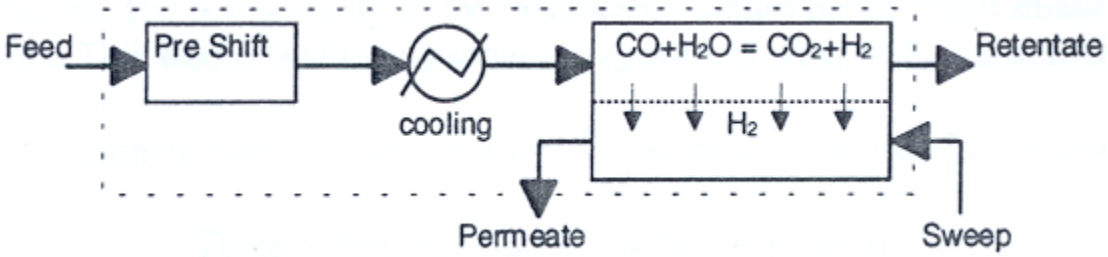

Figure 10. Schematic of staged membrane reactor system.

For heat and mass transfer devices, countercurrent operation is more efficient than concurrent operation. The latter is assumed here because of computational convenience: countercurrent simulation requires iteration on the guessed permeate exit flow to achieve convergence of the known inlet sweep condition. The assumption is conservative in that any increase in required reactor size requirements will tend to balance any decrease in reactor size from the equilibrium assumption. Damle et. al. (1994) have shown that the error incurred is only a couple percent at the high feed to permeate pressure ratios required for high CO conversion and hydrogen recovery.

Model Equations

The following two ordinary differential equations are solved:

$$\frac{dn_{dp}}{dx} = \frac{A_m}{L} \cdot N_P , \qquad \text{Eq. 3}$$

$$\frac{dH}{dx} = -h_{H2}(T) \cdot \frac{dn_{dp}}{dx} - \frac{Q_{loss}}{L} , \qquad \text{Eq. 4}$$

where n_{dp} is the moles of hydrogen transferred across the membrane, A_m is the membrane area, L is the reactor length, N_p is the hydrogen molar flux given by Eq. 2. In Eq. 4, Q_{loss} is the heat loss to the environment based on the user's fractional heat loss specification, H is the feed gas enthalpy, and $h_{H2}(T)$ is the molar enthalpy of hydrogen at the local temperature of the feed gas. The integration is performed numerically using a second order explicit predictor corrector method, and the adiabatic equilibrium is computed locally from the feed gas enthalpy and composition:

$$K(T) = \frac{n_{H2} \cdot n_{CO2}}{n_{CO} \cdot n_{H2O}} , \qquad \text{Eq. 5}$$

$$n_{CO} = n_{CO}^{\ o} - \xi , \qquad \text{Eq. 6}$$

$$n_{H2O} = n_{H2O}^{\ o} - \xi , \qquad \text{Eq. 7}$$

$$n_{CO2} = n_{CO2}{}^{o} + \xi \,, \qquad \text{Eq. 8}$$

$$n_{H2} = n_{H2}{}^{o} + \xi - n_{dp} \,, \qquad \text{Eq. 9}$$

$$H = \sum_i h_i(T) \cdot n_i \,, \qquad \text{Eq. 10}$$

where ξ is the extent of reaction variable, and n_i^o is the initial moles of species i. Eqs. 6-9 are substituted into Eq. 5 and the nonlinear equations Eq. 5 and 10 are solved with Newton's method for ξ and T. The moles of all reaction species are then updated using Eqs. 6-9. The equilibrium constant was curvefit to thermodynamic data of the relation $K(T) = \exp(-\Delta G^o_{rxn}/RT)$ to yield:

$$K(T) = 91607 \cdot T^2 + 1680 \cdot T - 1.6097, \quad (T \text{ in Kelvin}) \qquad \text{Eq. 11}$$

The sweep gas composition is updated at each point as the hydrogen permeates. Because there is no heat transfer over the membrane, the sweep temperature is only computed at the exit using the sweep composition and enthalpy computed from an energy balance over the unit.

Model Capabilities

The membrane reactor model can be run in one of two modes.

1) Specification of the reactor dimensions, and gas flow properties. The exiting gas streams are computed along with CO conversion, hydrogen recovery, superficial space velocity, and approximate unit footprint.
2) The second mode allows specification of a desired CO conversion, along with reactor dimensions. The required MR module length is output as a result, along with the required sweep flow rate.

The model allows evaluation of the effect of reactor dimensions, membrane thickness, steam to carbon monoxide ratio, as well as all gas exit properties on the required module dimensions and/or extent of reaction and hydrogen permeation. An appropriate user interface is under development in which default parameters will be provided.

Model Results

The following results were computed using the WGS membrane reactor. For this case, a pre-shift stage was included as shown in Figure 10. The input conditions and results are shown in Table 5. The inlet gas is that of Table 4, for a simulated gasifier product. The temperature and pressure of the inlet gas stream are taken from the Vision 21 flowsheet of Figure 2. The sweep gas temperature was arbitrarily set at 300 K. This temperature does not affect the calculations, but its value should be consistent with the tube size to give reasonable gas velocity. The sweep inlet velocity is shown in Table 5 and is proportional to the flow rate, temperature and inverse pressure. The sweep pressure is set at one atmosphere. This is the absolute (practical) minimum. The low sweep pressure allows a relatively high hydrogen concentration in the sweep gas. It is important to note that the membrane reactor only works so long as there is a hydrogen partial pressure driving force. Once the feed side hydrogen pressure matches that of the sweep gas, the WGS reaction is limited by the equilibrium composition. The primary purpose of the sweep gas is to dilute the hydrogen enough to provide a sufficient driving force over the

membrane, hence allowing high CO conversion. A feed-to-permeate pressure ratio of 15 atmospheres is typical (Bracht et. al., 1997).

Figures 11, 12 and 13 show profiles of temperature, gas composition, and CO conversion and pressure driving force over the length of the membrane reactor. As expected, the temperature increases due to the exothermic reaction. In Figure 11, the mole fraction of CO actually increases slightly in the first half of the unit because the total moles is decreasing (due to hydrogen permeation) faster than the CO. Note that the temperature (and CO conversion) are shown to begin higher than the MR inlet values specified in Table 5. Since the WGS reaction is adiabatic and occurs catalytically, reactions should not occur during external heat exchange, the gas at the inlet to the MR is not at equilibrium at the specified MR inlet temperature of 565 K. The equilibrium gas at the pre-shift reactor exit (higher temperature) has a lower conversion than at the lower MR inlet temperature, so the conversion increases quickly in the MR from 50% to 72%.

For a specified CO conversion, the reactor length and sweep gas flow rate are not independent. High sweep flow rates give a higher pressure driving force at the outlet (minimizing reactor length for a given conversion), but gives a highly diluted hydrogen product. Conversely, a very small pressure driving force maximized hydrogen concentration in the sweep, but results in a very long reactor. The compromise lies in specifying a minimum pressure driving force, computed from the position of the sharp "bend" in the CO conversion curve as the conversion levels off, as noted in the shape of the curves at the reactor exit in Figures 12-13.

Bracht et. al. (1997) give design characteristics for membrane reactors for IGCC applications. The dimensions used in the present simulation are based on these values. The membrane tube diameter is given as 10.4 cm, with a tube length of 2 m. The total number of modules is 3300, giving a membrane area of 2176 m^2. The catalyst volume is given as 25.3 m^3. These values assume a Knudsen diffusion membrane rather than a Pd membrane. These values compare reasonably well with the current values considering membrane differences and the unknown degree (if any) of conversion in the pre-shift reactor. The palladium membrane hydrogen flux depends exponentially on temperature. At the present reactor exit temperature, the Pd membrane used has an H_2 flux approximately 2.4 times that of Knudsen diffusion membranes quoted by Bracht.

Table 5. Sample simulation inputs and results.

Inputs	
Inlet Feed Gas Composition (vol % dry)	
CO	42.82%
H_2O	19.70%
H_2	27.42%
CO_2	8.34%
Other	1.72%
Temperature (K)	672
Pressure (atm)	15
Flow Rate (moles/s)	3312
Sweep Gas (N_2)	
Temperature (K)	300
Pressure (atm)	1
H_2O:CO ratio (inject steam)	*1*
Module Shell Diameter (cm)	15
Module Membrane Diameter (cm)	10
Number of Modules	1280
Specified CO Conversion (%)	95%
Membrane Thickness (micron)	10
Specified MR Inlet Temperature (K)	565
Specified Heat Loss (%)	0
Results	
H_2 Recovery	96.14%
MR Length (m)	2.2
Total Membrane Area (sq. m)	925
Intermediate Heat Transfer (kW)	42,158
MR Footprint (sq. ft)	309
Pre-Shift CO Conversion (%)	49.5%
Pre-Shift Reactor Exit Temperature (K)	852
Sweep Gas Flow Rate (moles/s)	17416
H_2 Concentration in Sweep (vol %)	11%
Inlet Sweep Velocity (m/s)	42.7

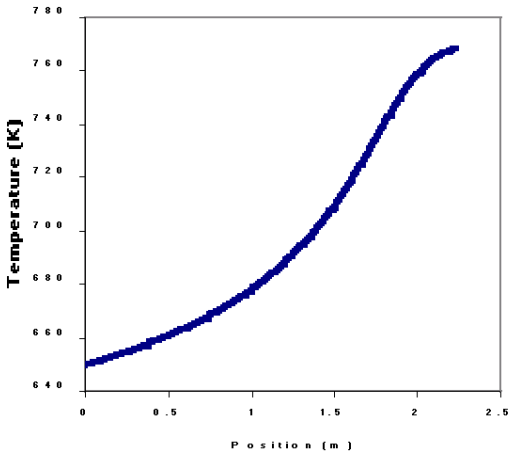

Figure 11. Temperature profile.

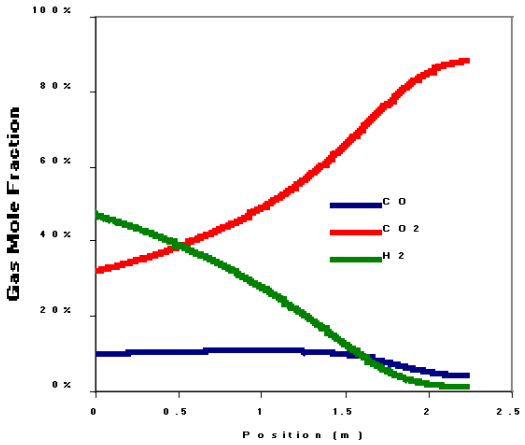

Figure 12. Gas composition profiles.

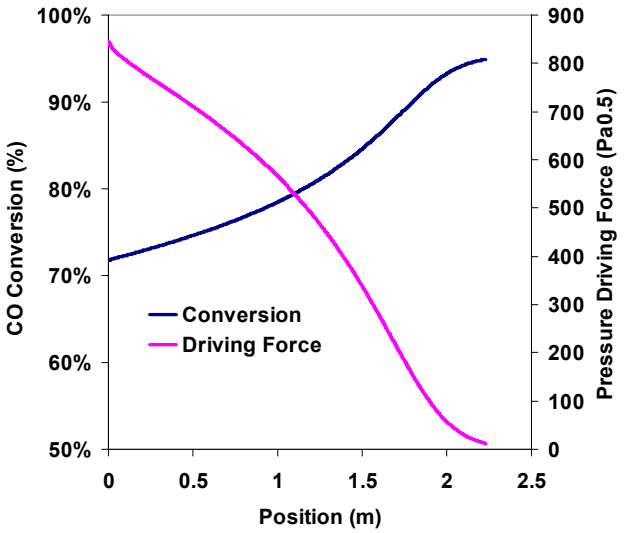

Figure 13.CO conversion and pressure driving force.

Summary of Current Model Status

A one-dimensional membrane reactor for the water gas shift reaction has been developed and tested. The membrane reactor converts the CO in cleaned syngas to hydrogen over a catalyst and simultaneously separates the hydrogen by permeation through a palladium-based membrane. The reactor is placed downstream of the gas cleanup units and prior to fuel cells, combustors or other process equipment. The model assumes hydrogen permeation is slower than chemical reaction and chemical equilibrium is assumed throughout the reactor. A sweep gas is required to remove the hydrogen and is assumed to flow concurrently to the feed gas.

The model can be run in two stages with intercooling in between to maintain catalyst operating temperatures and minimize membrane size and costs. The model allows calculation of CO conversion, H_2 recovery, sweep gas flow rate, and required heat transfer (for staged operation). The effects of reactor dimensions, number of parallel modules, membrane thickness, steam-to-CO ratio, and heat losses on the reactor performance can be tested. Alternately, the model can compute the required reactor length and sweep flow rate for a desired CO conversion.

A standalone version of the model has been completed. During the next quarter a user interface will be developed and the model will be integrated into the Vision 21 computational workbench.

Results and Discussion

During the last quarter we have continued development of the CFD models for the entrained flow gasifiers and have performed overall plant simulations using the Vision 21 Workbench. Details are provided below.

Vision 21 Workbench Calculations

In the last quarterly report [Bockelie et al, 2003a], we described a set of simulations performed to evaluate the Vision 21 workbench for two gasifier types (1 and 2 stage slurry fed gasifiers) burning two different coals (i.e., Illinois #6, Petcoke). Comparisons of the overall plant efficiency and power generation predicted with the workbench as compared to predicted values from the DOE Vision 21 configuration showed good agreement. However, in the DOE studies it was assumed that the gasifier operated with 84% cold gas efficiency, whereas the models had lower cold gas efficiency.

During the last performance period, two additional energy plant simulations have been performed.

- The first gasifier simulation used a two stage slurry feed gasifier that was modified to improve the fuel burnout and therefore achieve ~84% cold gas efficiency. The improved burnout was obtained by increasing the height of the second stage (i.e., overall L/D = 11 instead of L/D=6) to provide more residence time for char gasification (see below for more details). For this gasifier configuration the gasifier process conditions were the same as in the previously reported results [Bockelie et al, 2003a] and are briefly summarized in Tables 6 and 7.

- The second gasifier simulation utilized a one stage, dry feed, up-flow gasifier. Here, we used the gasifier geometry and process conditions from the one stage, dry feed, up-flow gasifier reported in [Bockelie et al, 2002]; the process conditions are summarized in Tables 6 and 7. Note that the “dry feed” is transported using nitrogen. In addition, no additional steam was used to temper the gasification process or improve gasifier cold gas efficiency.

Table 6. Fuel Properties

	Illinois #6
Proximate Analysis	As-Received (wt%)
Moisture	11.12
Ash	9.70
Volatile Matter	34.99
Fixed Carbon	44.19
TOTAL	100.00
HHV (Btu/lb)	11666
Ultimate Analysis	As-Received (wt%)
Moisture	11.12
Carbon	63.75
Hydrogen	4.50
Nitrogen	1.25
Sulfur	2.80
Ash	9.70
Oxygen (by difference)	6.88
TOTAL	100.00

Table 7. Gasifier Process Conditions

Item	2 Stage slurry feed	1 Stage dry feed
Fuel Flow Rate (tpd)	3000	2600
Slurry – wt % (dry basis)	66 %	--
N2:Coal (lb:lb)	--	0.075
Oxidant Flow Rate (tpd)	2200	2900
Feed Temperature (K)	422	475
Oxidant Temperature (K)	452	475

The Vision 21 network of modules used to perform the simulations is the same as shown in Figure 4 of [Bockelie et al, 2003a]. The simplifying assumptions for the gas clean up system, flue gas recycle and downstream equipment process conditions were repeated for the current study. Likewise, for equipment other than the gasifier, inputs for the associated component model were taken directly from the reference configuration; in situations where data was not provided, data from similar units was used or the component was configured to obtain the proper results for the "baseline" simulation. The inputs for these components were not changed for subsequent simulations. As a result, some downstream equipment might not be configured to operate in an optimal manner for the non-baseline simulations.

Results – Workbench Simulations

Illustrated in Figures 14-15 are the results of the workbench simulations using CFD models for the gasifiers and process conditions described above. Shown in Figure 14 is the predicted overall plant efficiency. Illustrated in Figure 15 is the predicted net power for the principal power producing components. In these figures, the results labeled "DOE Baseline", "2 Stage L/D=6", "2 Stage L/D=11" and "1 Stage Dry Feed" refer to, respectively, values from the DOE Vision 21 configuration flow sheet in Figure 2, a two stage slurry feed up flow gasifier with a L/D=6 geometery, a taller two stage slurry feed up flow gasifier with a L/D=11 and a one stage dry feed up flow gasifier.

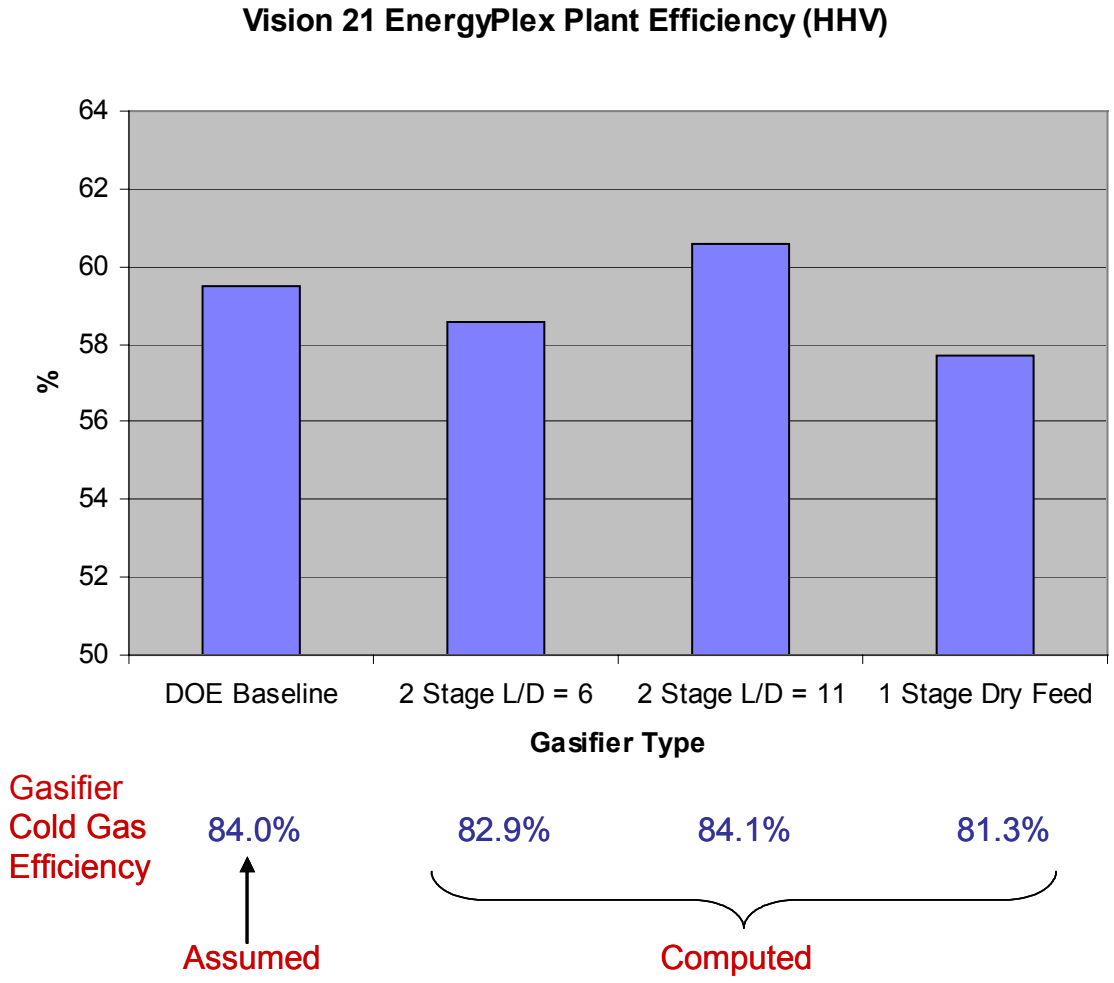

Figure 14. Vision 21 Workbench Simulation Results – Plant Efficiency.

Several items can be seen from the plots in Figure 14. First, the overall plant efficiency as calculated by the workbench is in good agreement with the DOE values. Note that the Vision 21 target value of 60% is achieved with a slurry feed gasifier with a cold gas efficiency of 84.1%. The overall plant efficiency falls to just below 60% for the gasifier achieving 82.9% cold gas efficiency. The difference in these two predictions is the length of the two-stage gasifier. The

82.9% case was obtained with a gasifier length-to-diameter ratio of 6. The 84.1% cold gas efficiency was obtained by increasing the gasifier length-to-diameter ratio to 11, thereby increasing the coal burnout. Note that for the one stage dry feed gasifier the overall plant efficiency is somewhat less than the DOE Baseline and the slurry feed gasifiers, indicating a need to re-define the process conditions to use with this gasifier to obtain higher efficiencies.

It should be noted that the gasifier cold gas efficiency shown in Figures 14 and 15 is a computed value for the workbench simulations but an *assumed* value in the DOE information. The computed cold gas efficiency for the models appears to have the expected trend: the two stage gasifier has a higher cold gas efficiency than the one stage gasifier, even with a dry feed in the one stage case.

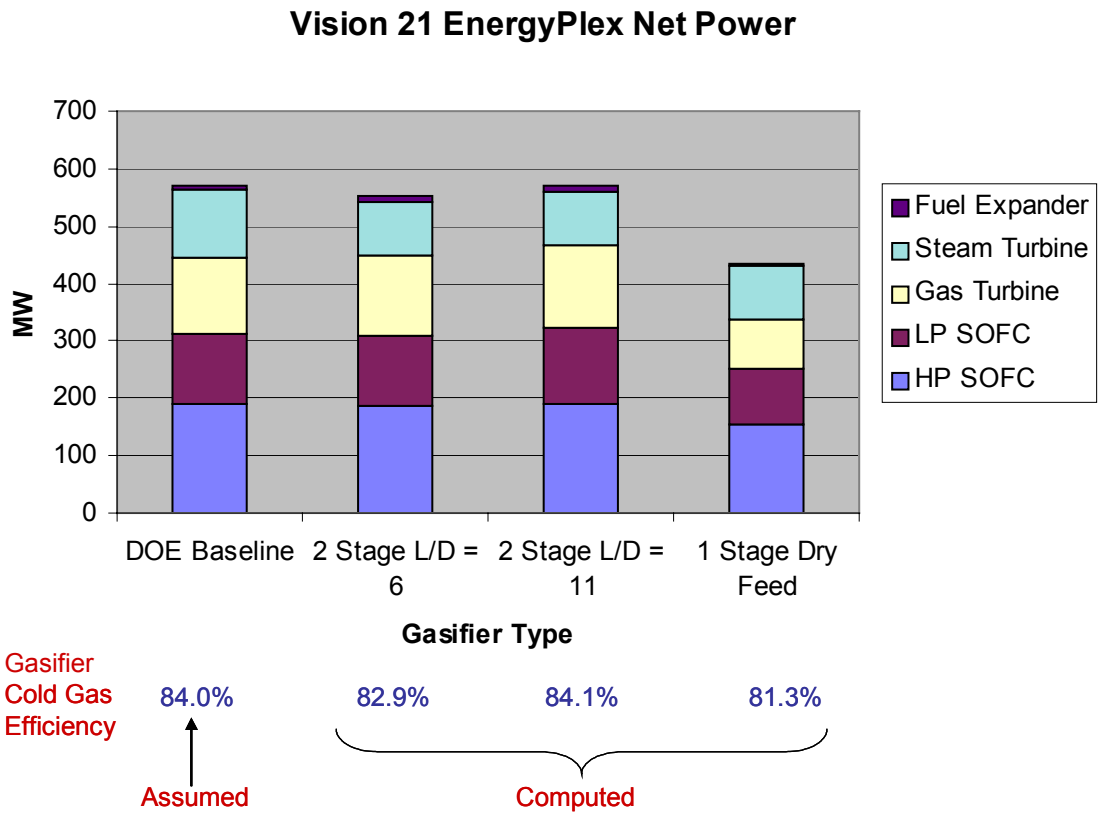

Figure 15. Vision 21 Workbench Simulation Results – Net Power generated by main components.

Comparing the Net Power results in Figure 15, again there is good agreement between DOE provided values and the workbench calculated values. The power generated with the dry feed gasifier configuration is due to using a lower coal feed rate.

Based on the above results, additional simulations of interest would be to investigate a one and a two stage dry feed gasifier that provides comparable Net Power as for the DOE baseline. Here, we are assuming that the dry feed will provide better efficiency due to not having to boil away the liquid slurry. In addition, it would be interesting to determine the impact of using CO2 instead of N2 as the fuel transport fluid in a dry feed system.

In the following section we briefly summarize a CFD simulation for the one stage gasifier (L/D=11) that was performed as part of the workbench simulations discussed above.

Results – Two Stage CFD Gasifier Model

The gross gasifier geometry used for these simulations is summarized in Figure16. Note that the gasifier modeled here is about twice the height than that used in previous simulations. The process conditions are based on the Vision 21 reference configuration and have been described above. The flow distributions by injector level are the same as used in previous simulations of this gasifier [Bockelie et al, 2003a]: all of the oxidant and 78% of the coal is uniformly distributed amongst the fuel injectors in the first stage and the remaining coal is uniformly distributed across the injectors in the second stage. No oxidant is injected into the upper stage. For firing the Illinois #6 coal, the overall oxygen:carbon (O_2:C) mole ratio is ~0.40, resulting in an overall stoichiomery of about ~0.48 and a stoichiometry in the lower stage of about ~0.62.

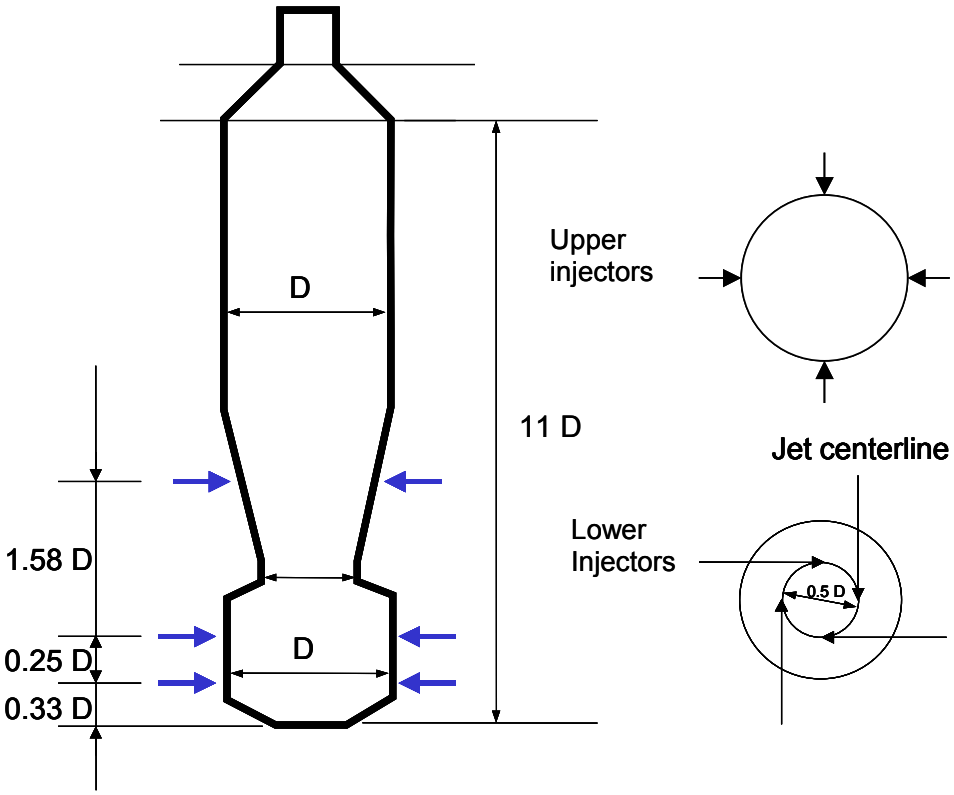

Figure 16. Schematic of Two-Stage Up Flow configuration.

Illustrated in Figure 17 are the average values of the gas temperature and main gas species as a function of elevation within the gasifier for the L/D=6 and L/D=11 gasifier simulations. As can be seen from the figure, the predicted values are in good agreement within the lower section of the gasifier where the simulations should overlap.

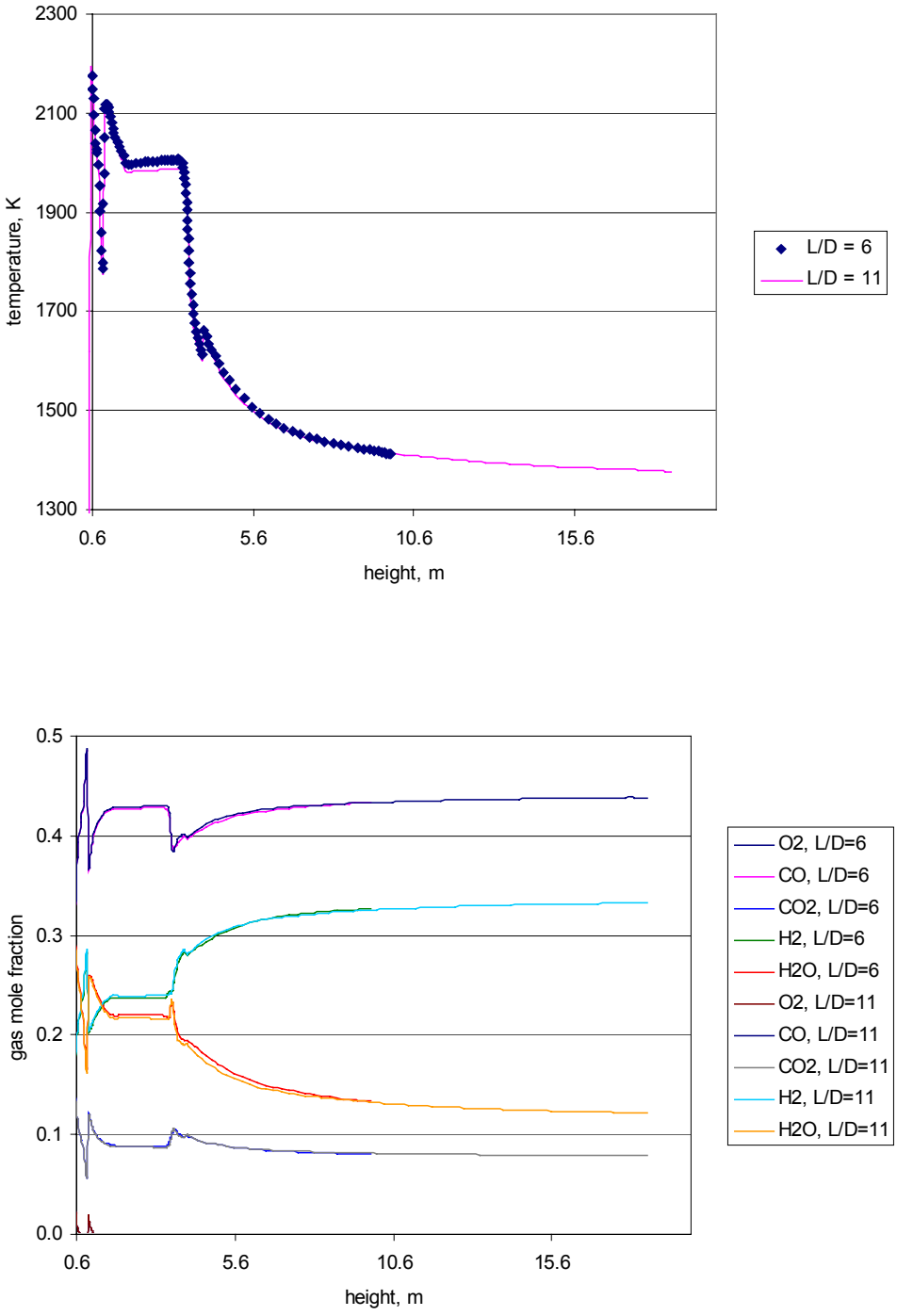

Figure 17. Average gas temperature and major gas species concentration as a function of gasifier elevation for two stage slurry feed gasifiers with overall height to diameter ratios of L/D=6 and L/D=11.

Listed in Table 8 are the average gasifier exit values for gasifiers with L/D=6 and L/D=11. Note that there is only a modest change in the average values by adding the additional height (residence time) to the gasifier. As expected, the taller gasifier has slightly greater carbon conversion, lower gas temperature and higher cold gas efficiency.

Table 8. Two Stage Gasifier Results.

L/D	6	11
Exit Temperature, K	1412	1377
Carbon Conversion, %	91.4	94.6
Exit LOI, %	34.15	9.37
Deposit LOI, %	47.88	45.05
Deposition, %	8.51	8.36
PFR Residence Time, s	0.83	1.74
Particle Residence Time, s	0.37	0.69
Mole Fraction: CO	43.3%	43.8%
H_2	32.7%	33.3%
H_2O	13.3%	12.2%
CO_2	8.1%	7.9%
H_2S	0.8%	0.8%
COS	0.0%	0.0%
N_2	1.6%	1.6%
Exit Mass Flow, klb/hr	497	502
HHV of Syngas, Btu/lb	4988	5092
HHV of Syngas, Btu/SCF	248	254
Cold-Gas Efficiency, %	82.9	84.2

Preliminary Gasifier Calculations - *AIOLOS*

The work during the last performance period has been focused on the steady-state and time-dependent simulation of a Two-Stage industrial gasifier configuration (see Figure 18). The time-dependent simulation modeled a start-up scenario for the configuration under consideration.

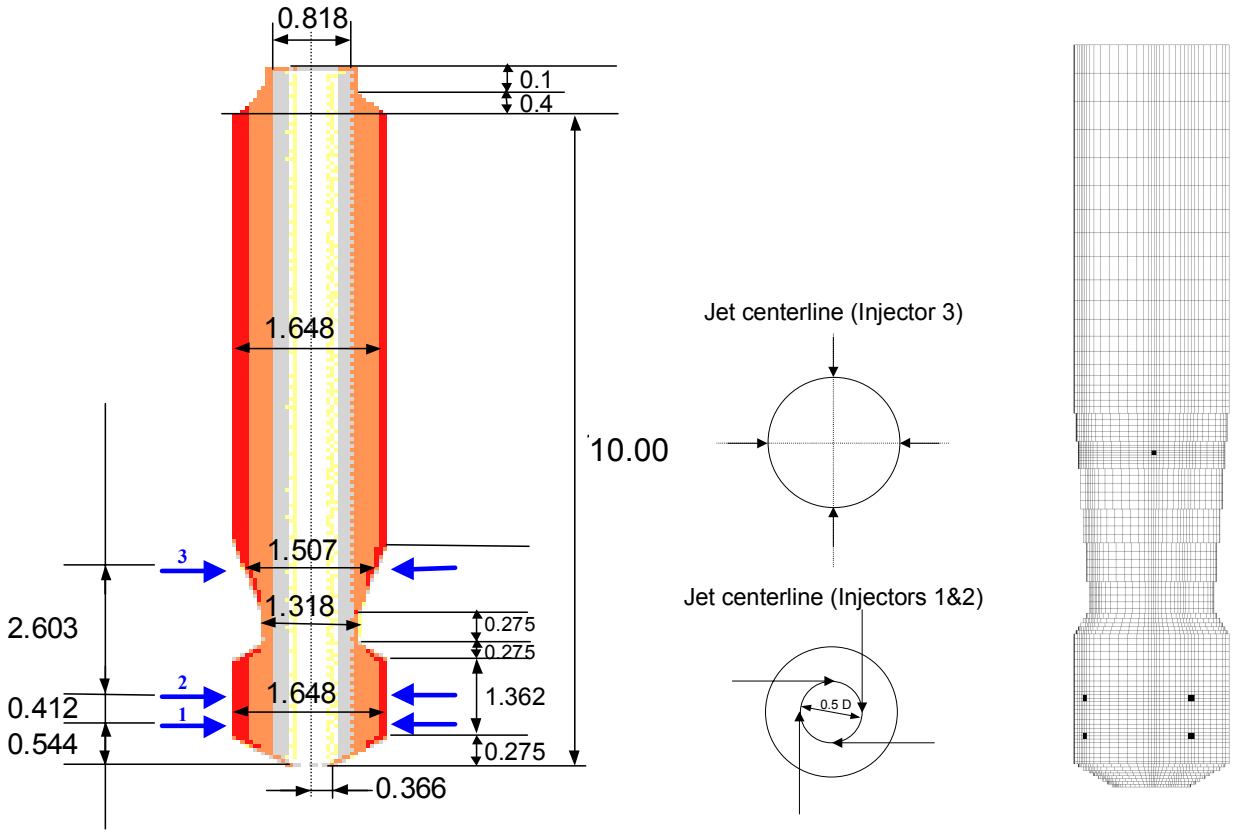

Figure 18: Two-Stage Industrial Gasifier Configuration (Left) and Geometry Model (Right)

Steady state results have been generated for the following operating conditions using an Illinois coal #6 (see Table 9) with a uniform size 39.8 μm as the base fuel:

Coal flow rate:	32.274 kg/s
O_2 (95% vol.) and N_2 (5% vol.) flow rate:	23.128 kg/s
H_2O (for wet slurry) flow rate:	11.188 kg/s
Gasifier pressure:	18 atm
Inlet coal temperature:	422 K

Inlet O_2 temperature: 475 K

Table 9: Fuel properties of Illinois coal #6

Proximate Analysis	As-Received (wt-%)
Volatile Matter	34.99
Fixed Carbon	44.19
HHV (Btu/lb)	11666
Ultimate Analysis	As-Received (wt-%)
Carbon	63.75
Hydrogen	4.50
Nitrogen	1.25
Sulfur	2.90
Moisture	11.12
Ash	9.7
Oxygen	6.78

Steady state results have been generated assuming a completely dried coal with 100 % vaporized slurry water. Furthermore, the injectors have been modeled assuming ideal mixing between the streams. Results showing average profiles of major species concentrations, and average temperature over gasifier height are shown in Figures 19 and 20. The gasifier exit conditions predicted with AIOLOS are summarized in Table 10 and compared to the corresponding GLACIER simulations performed by REI.

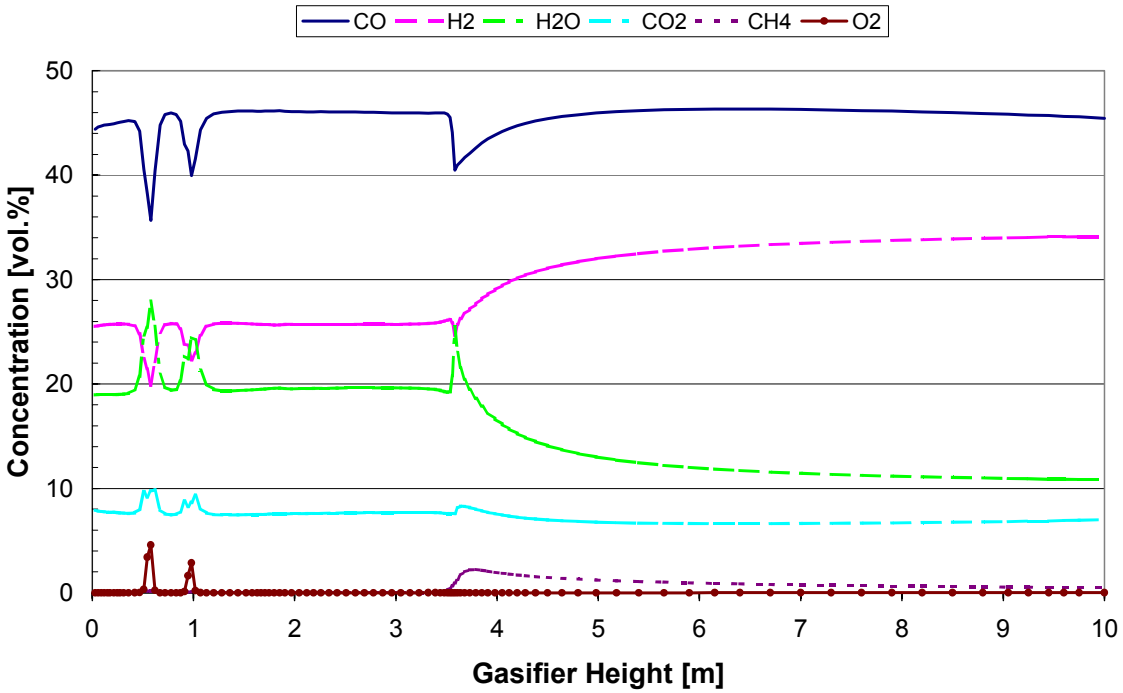

Figure 19: Average profiles of major species concentrations over gasifier height.

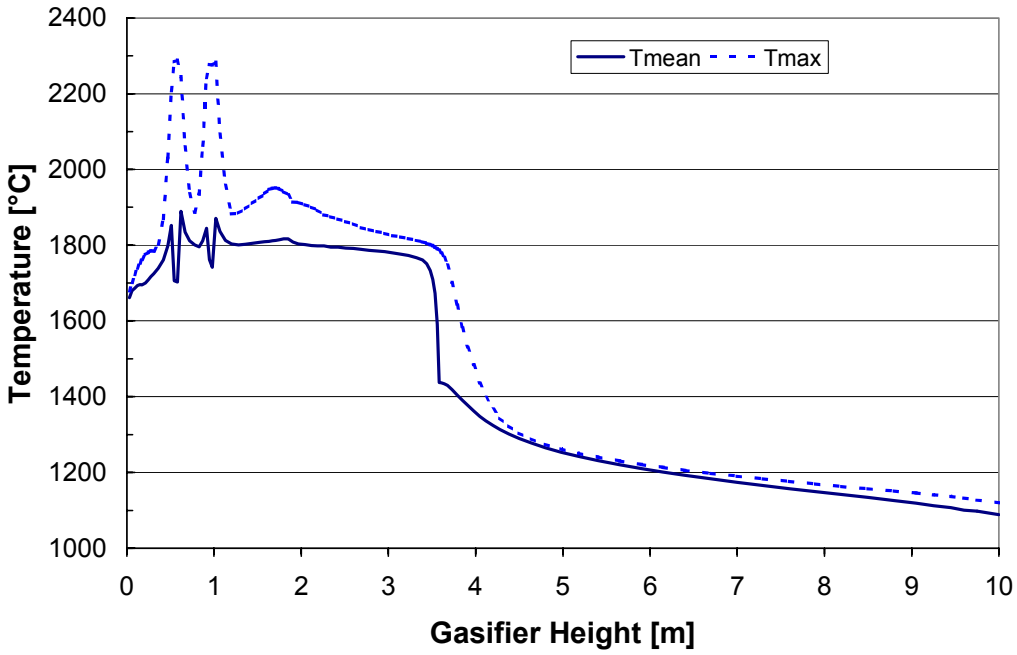

Figure 20: Profiles of average and peak temperature over gasifier height.

Table 10: Two-Stage gasifier exit conditions predicted by AIOLOS and GLACIER

	AIOLOS	GLACIER
CO-Concentration	45.5 Vol.-%	43.0 Vol.-%
H2-Concentration	34.1 Vol.-%	32.3 Vol.-%
H2O-Concentration	10.9 Vol.-%	14.0 Vol.-%
CO2-Concentration	7.0 Vol.-%	8.2 Vol.-%
CH4-Concentration	0.5 Vol.-%	0.18 Vol.-%
O2-Concentration	0.0 Vol.-%	0.00 Vol.-%
Heating Value and Mass Flow	12260 kJ/kgGas (62.61 kgGas/s)	11499 kJ/kgGas (62.57 kgGas/s)
Cold Gas Efficiency	87.5 %	82.2 %

A start-up scenario going from 50 %-Load to 100 %-Load by increasing the load in 10 % increments has been defined and modeled. The starting conditions used were determined to air (23.3 wt.-% O_2 and 76.7 wt.-% N_2) at a pressure of 18 atm and a temperature of 1,000 °C. The 100 %-Load settings of the steady state analysis were used to determine the 50 %-100 %-Load gasification conditions by simply reducing all the mass flows according to the load:

The time marching arrangement summarized in Table 11 has been used to simulate the start-up scenario:

Table 11: Time marching arrangement for the Two-Stage gasifier start-up scenario

Load	Time	Time Steps	Δt	Iterations	SX5-CPUh
50 %	0.0 - 0.5 s	50	0.01 s	250,000	18.50
50 %	0.5 - 1.5 s	50	0.02 s	300,000	22.20
50 %	1.5 - 4.0 s	50	0.05 s	600,000	44.40
50 %	4.0 - 4.5 s	5	0.10 s	110,000	08.14
50 %	4.5 - 5.5 s	5	0.20 s	110,000	08.14
50 %	5.5 - 10.5 s	10	0.50 s	400,000	29.60
50 %	10.5 - 20.5 s	10	1.00 s	450,000	33.30
60 %	20.5 – 21.5 s	10	0.10 s	200,000	14.80
60 %	21.5 – 26.5 s	10	0.50 s	400,000	29.60
60 %	26.5 – 31.5 s	5	1.00 s	225,000	16.65
70 %	31.5 – 32.5 s	10	0.10 s	200,000	14.80
70 %	32.5 – 37.5 s	10	0.50 s	400,000	29.60
70 %	37.5 – 42.5 s	5	1.00 s	225,000	16.65
80 %	42.5 – 43.5 s	10	0.10 s	200,000	14.80
80 %	43.5 – 48.5 s	10	0.50 s	400,000	29.60
80 %	48.5 – 53.5 s	5	1.00 s	225,000	16.65
90 %	53.5 – 54.5 s	10	0.10 s	200,000	14.80
90 %	54.5 – 59.5 s	10	0.50 s	400,000	29.60
90 %	59.5 – 64.5 s	5	1.00 s	225,000	16.65
100 %	64.5 – 65.5 s	10	0.10 s	200,000	14.80
100 %	65.5 – 67.5 s	5	0.50 s	200,000	14.80
100 %	67.5 – 68.5 s	1	1.00 s	45,000	03.33
Total	68.5 s	296		5,965,000	441.41

In the applied time marching arrangement (see Table 11) time steps ranging from 0.01 s to 1 s have been used to describe the process. An iterative SIMPLE method requiring 5,000 (Δt = 0.01s) to 45,000 iterations (Δt = 1 s) per time step was applied to converge each time level. A total number of 296 time steps covering 68.5 real-time second have been computed requiring a total number of 5,965,000 iterations. The calculations have been performed on a Vector Supercomputer (NEC SX5) consuming a total number of 441.41 SX5-CPUh. If the same simulation were to be performed on a more affordable machine, such as a sixteen CPU Linux cluster, we estimate that the same simulation would require ~170hrs of continuous compute time.

In the startup simulation, 20.5 real time seconds were modeled for the initial 50 %-Load increase to reach acceptable steady state conditions. In order to reduce the computational expenditure for the entire calculation it has been decided to calculate a constant time period of 11 s on each load level before switching to the next load level (disregarding the fact that this might be too short to achieve steady state conditions on every load level).

The transient results are exemplified in Figures 21-36, which show time-dependent temperature and CO values for the 50 %-Load start-up. The results after 0.2 s (Figures 21 and 22) show a deep jet penetration into the center region of the geometry in the second stage. The jets in the first stage tend to build a concentric ring along the gasifier wall. In the following 0.2 s (Figures 23-26) the rotating flow from the first stage reaches the second stage and produces a CO rich center region and very high local temperatures in the geometry and at the furnace walls. In the following 0.6 s (Figures 27-34) the center CO bubble from the second stage moves downwards into the center part of first stage producing a homogenous well-mixed CO-field in the bottom part of the gasifier. At the same time the near wall flow from the first stage is moving upwards to the gasifier exit. During this process local temperatures can reach very high values > 2500 °C. After 2 s the entire gasifier is filled with a homogenous CO-level with some peak areas in the bottom part of the gasifier (Figures 35 and 36). In the subsequent time the CO level slowly increases to the steady state value that is reached at time level 20.5 s (see movie-file 2Stage-T-50-100%Load.mpg).

More detailed results are available in the corresponding movie-files:

- 2Stage-T-50-100%Load.mpg
- 2Stage-CO-50-100%Load.mpg
- 2Stage-CO2-50-100%Load.mpg
- 2Stage-O2-50-100%Load.mpg
- 2Stage-H2-50-100%Load.mpg

A copy of these movie files has been provided to our DOE program officer.

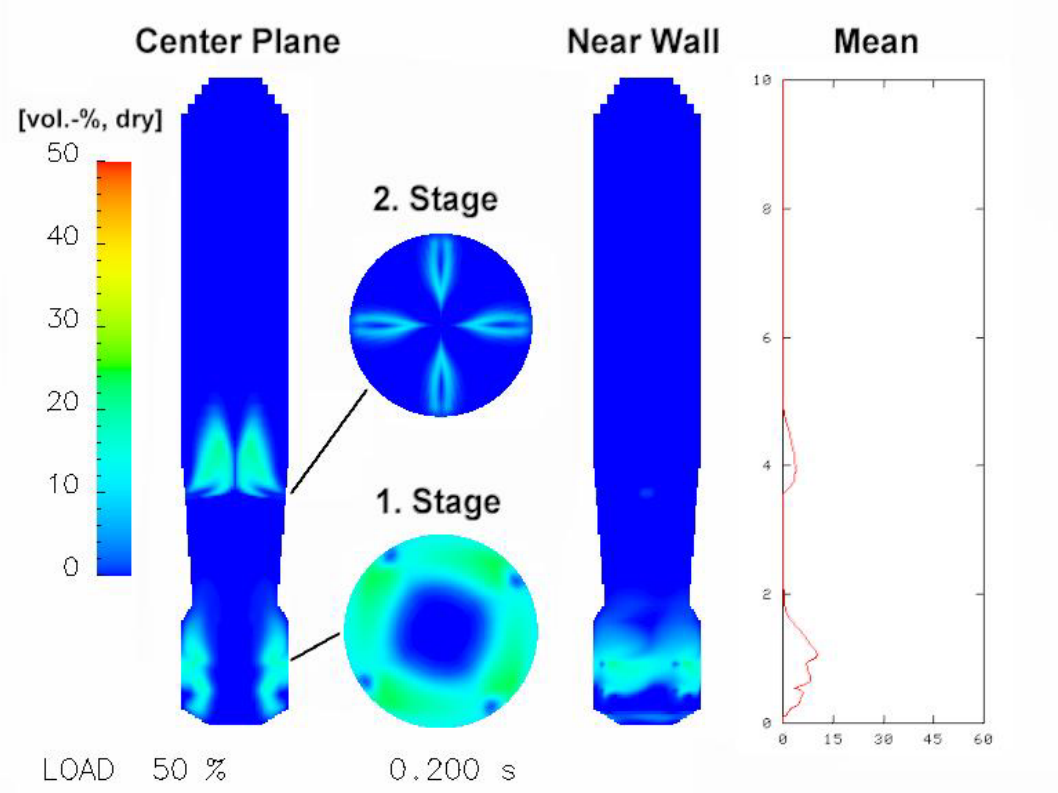

Figure 21: Computational results of inner, near wall, and mean CO-concentrations (t = 0.2 s)

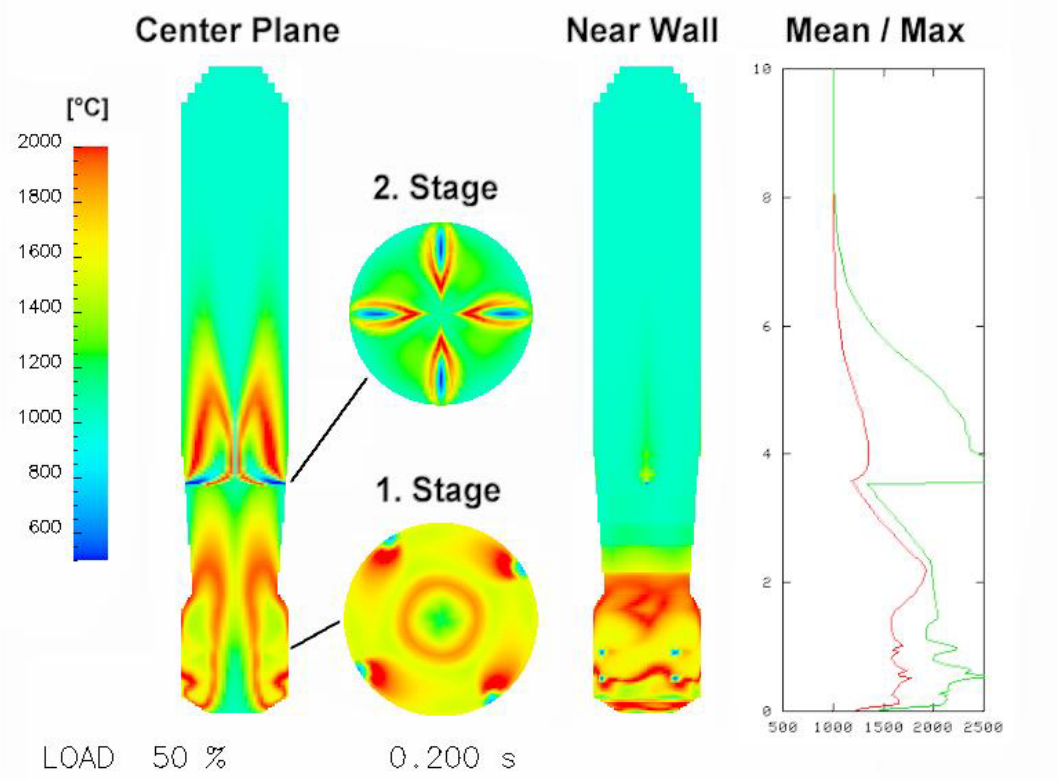

Figure 22: Computational results of inner, near wall, and mean temperature (t = 0.2 s)

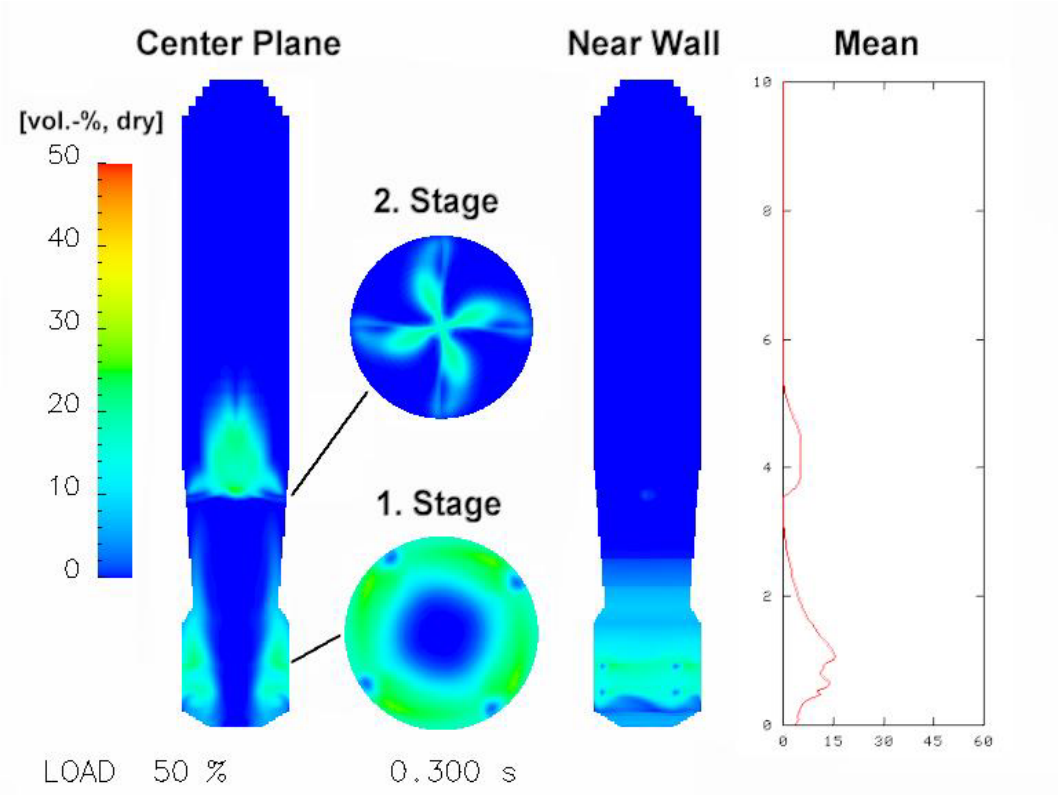

Figure 23: Computational results of inner, near wall, and mean CO-concentrations (t = 0.3 s)

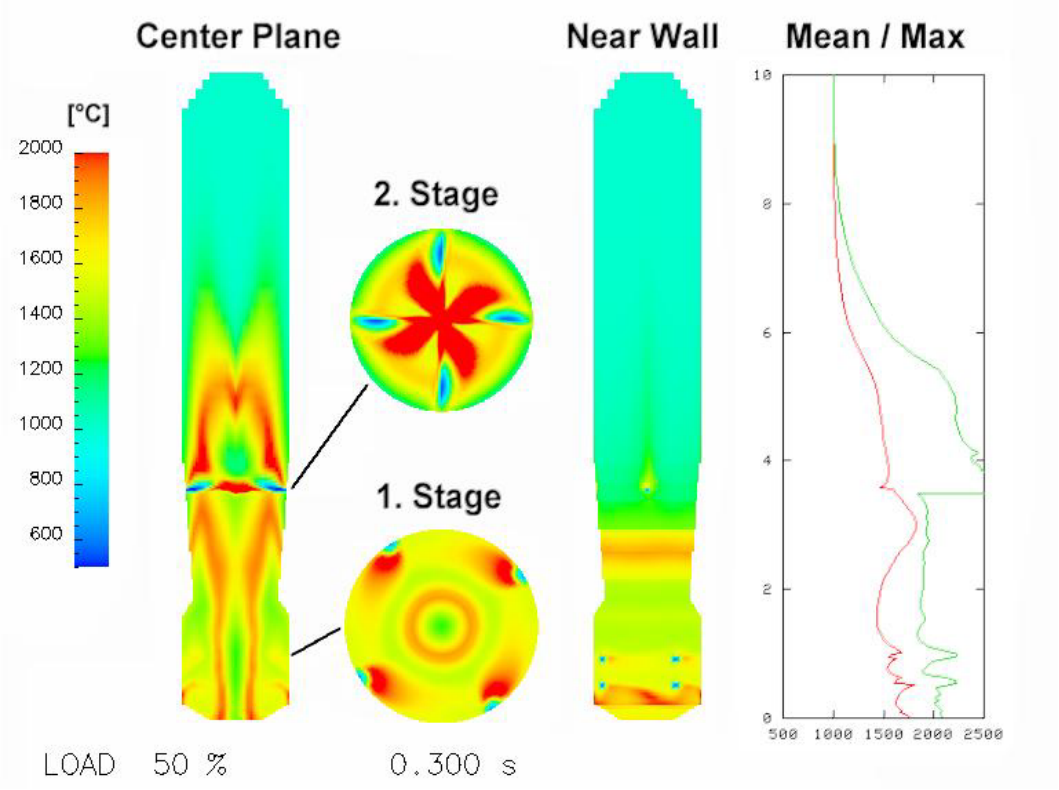

Figure 24: Computational results of inner, near wall, and mean temperature (t = 0.3 s)

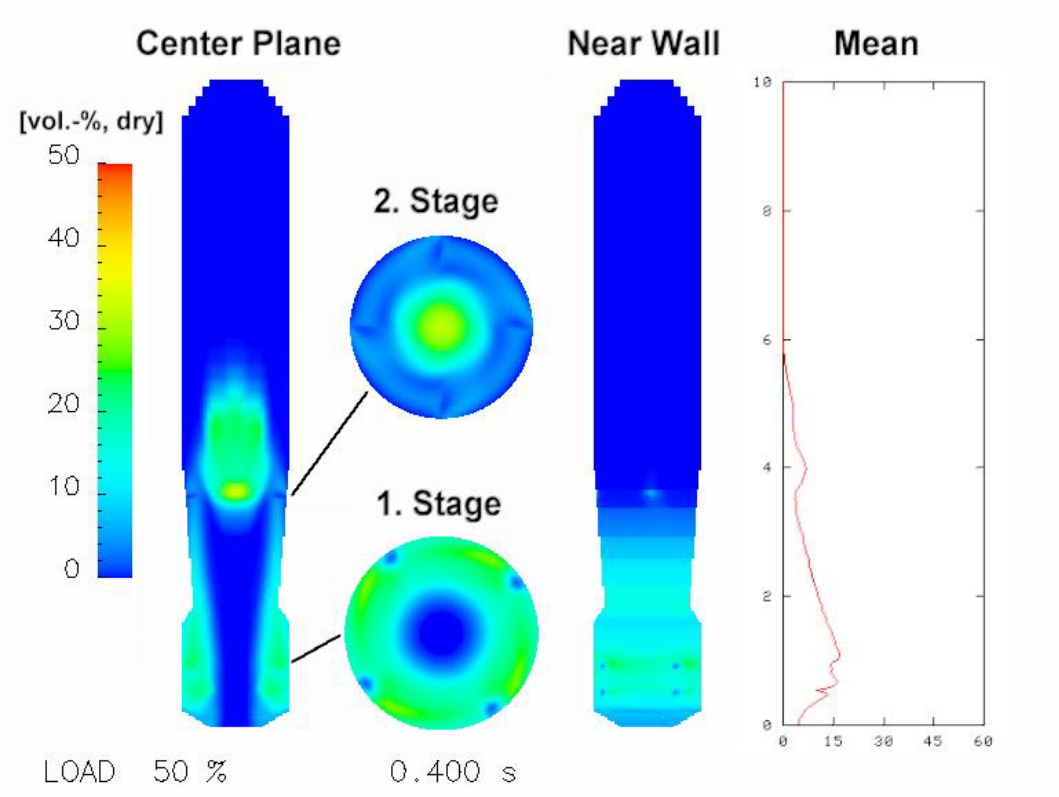

Figure 25: Computational results of inner, near wall, and mean CO-concentrations (t = 0.4 s)

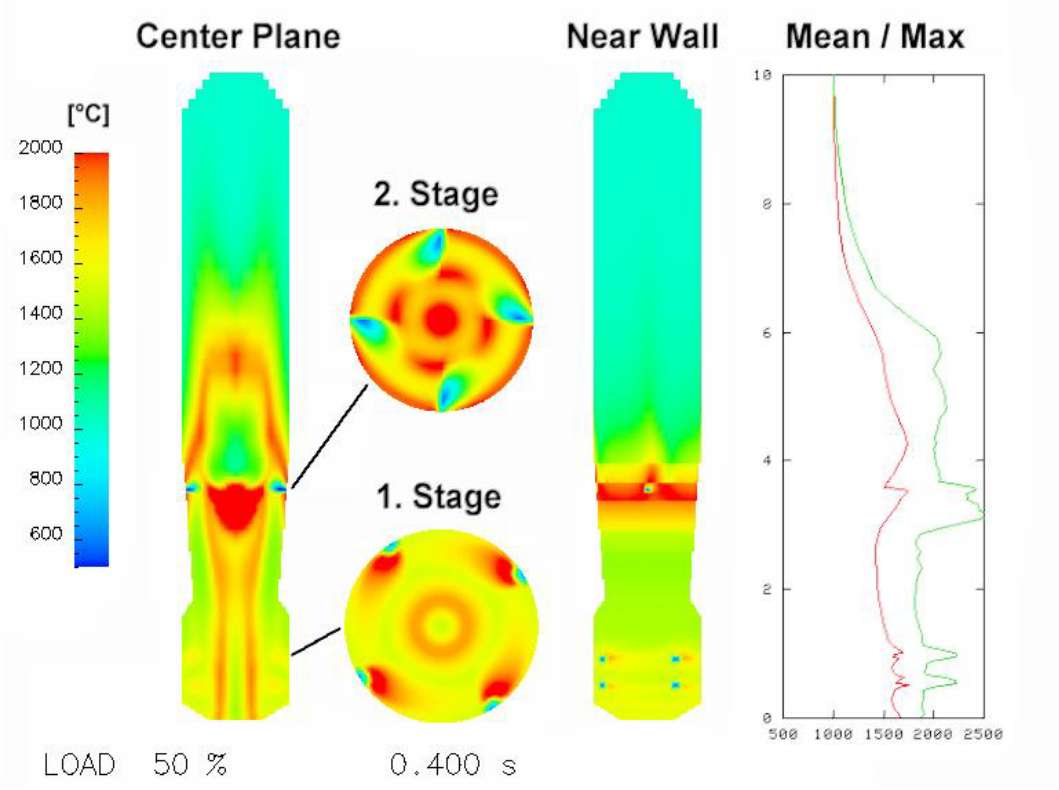

Figure 26: Computational results of inner, near wall, and mean temperature (t = 0.4 s)

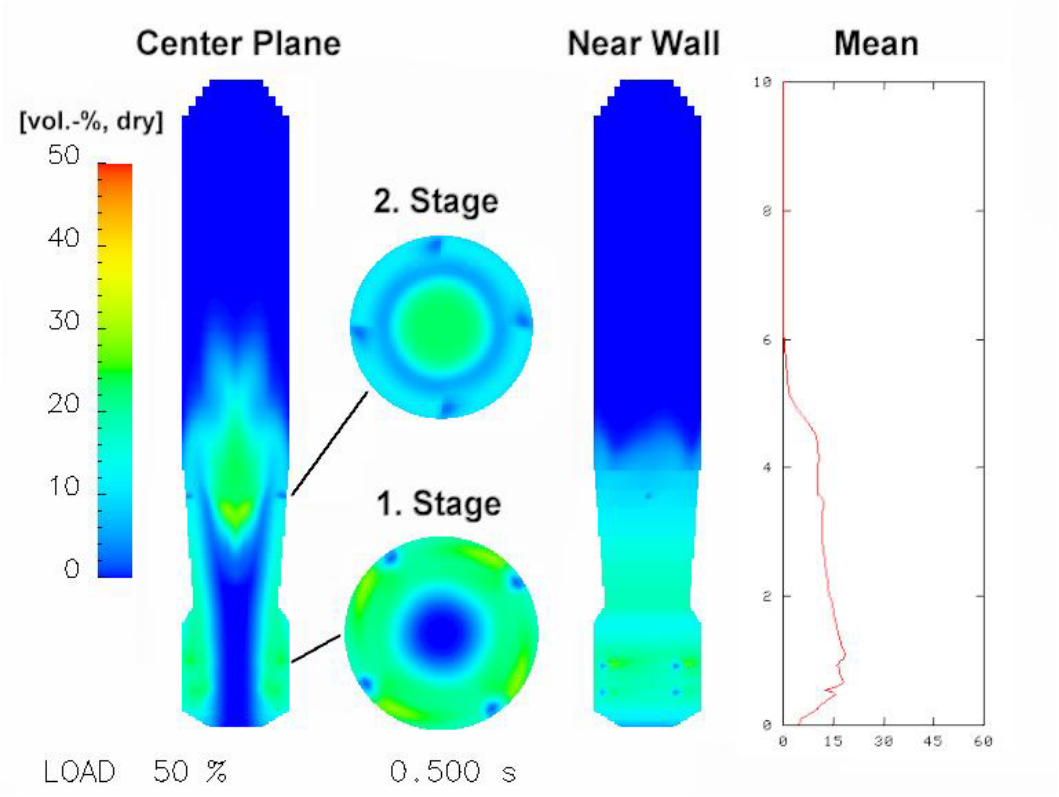

Figure 27: Computational results of inner, near wall, and mean CO-concentrations (t = 0.5 s)

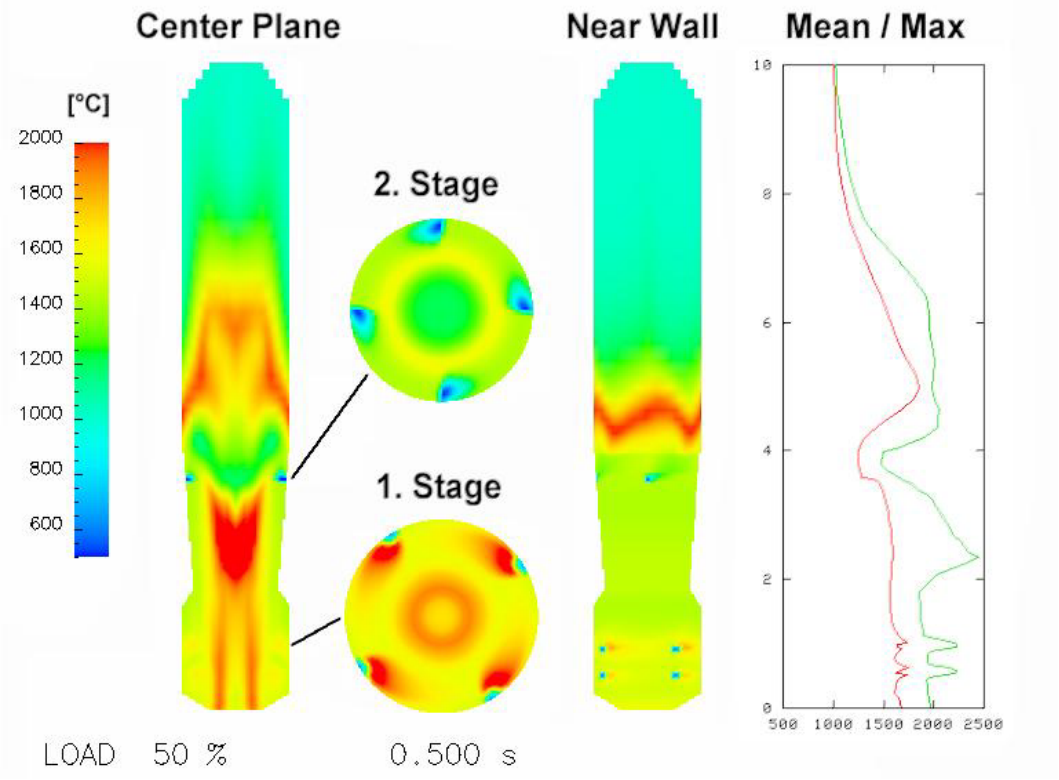

Figure 28: Computational results of inner, near wall, and mean temperature (t = 0.5 s)

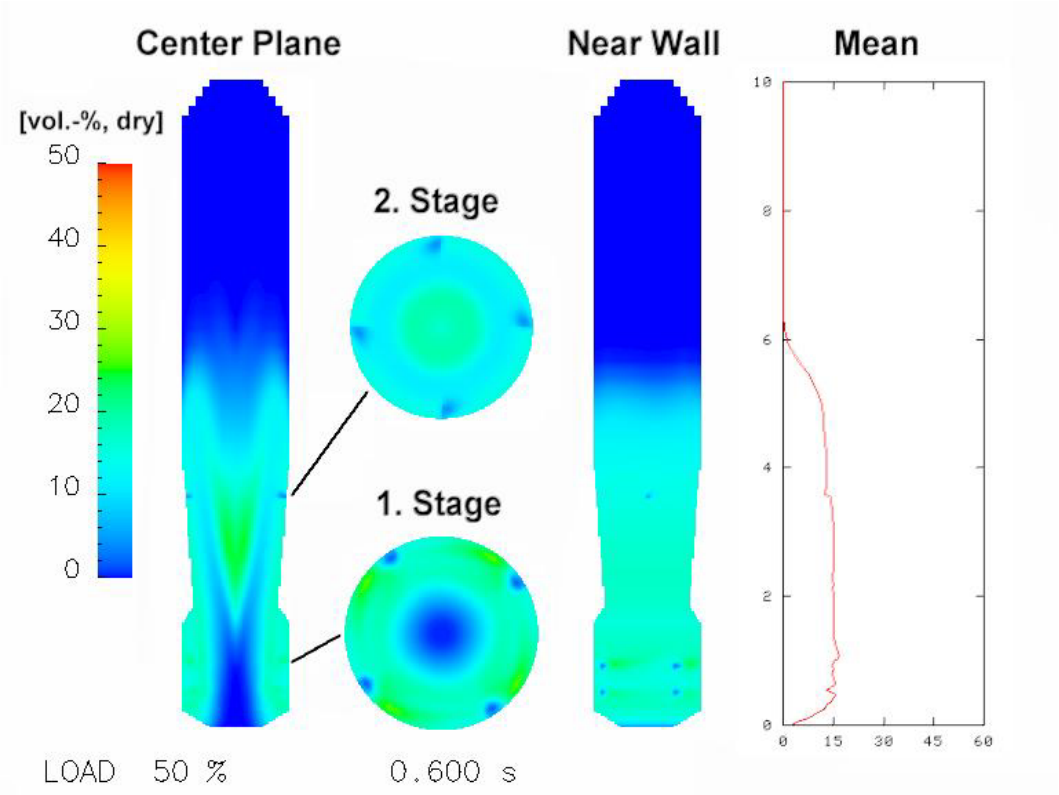

Figure 29: Computational results of inner, near wall, and mean CO-concentrations (t = 0.6 s)

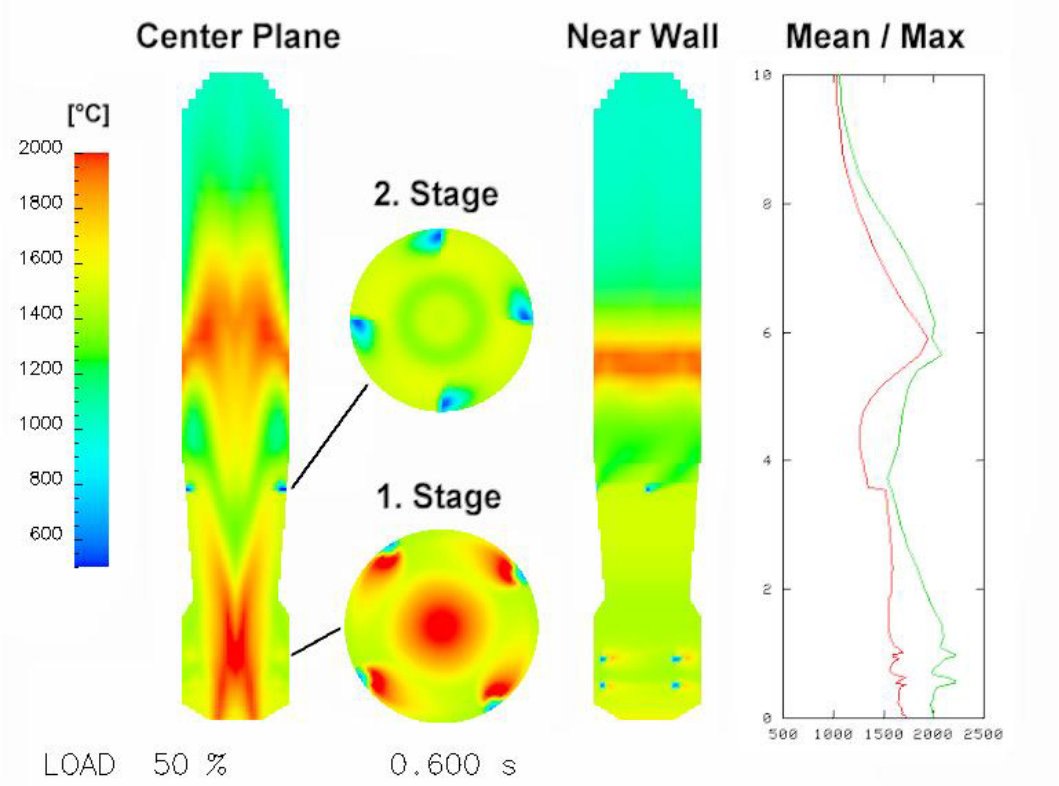

Figure 30: Computational results of inner, near wall, and mean temperature (t = 0.6 s)

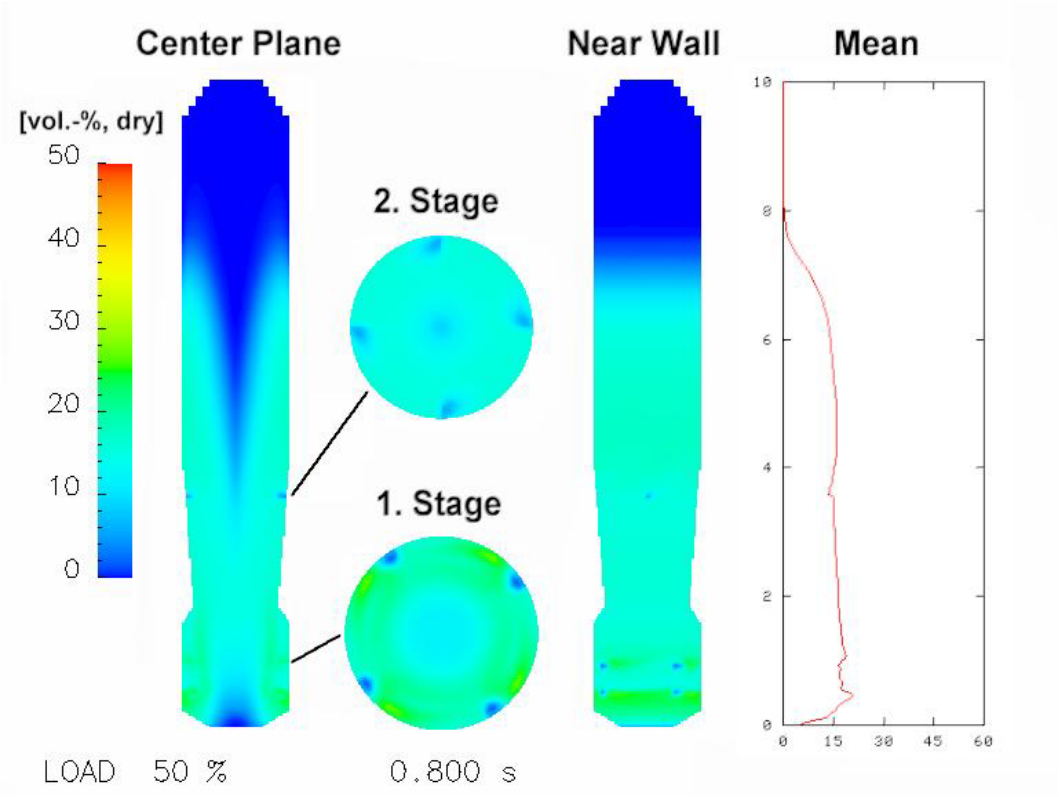

Figure 31: Computational results of inner, near wall, and mean CO-concentrations (t = 0.8 s)

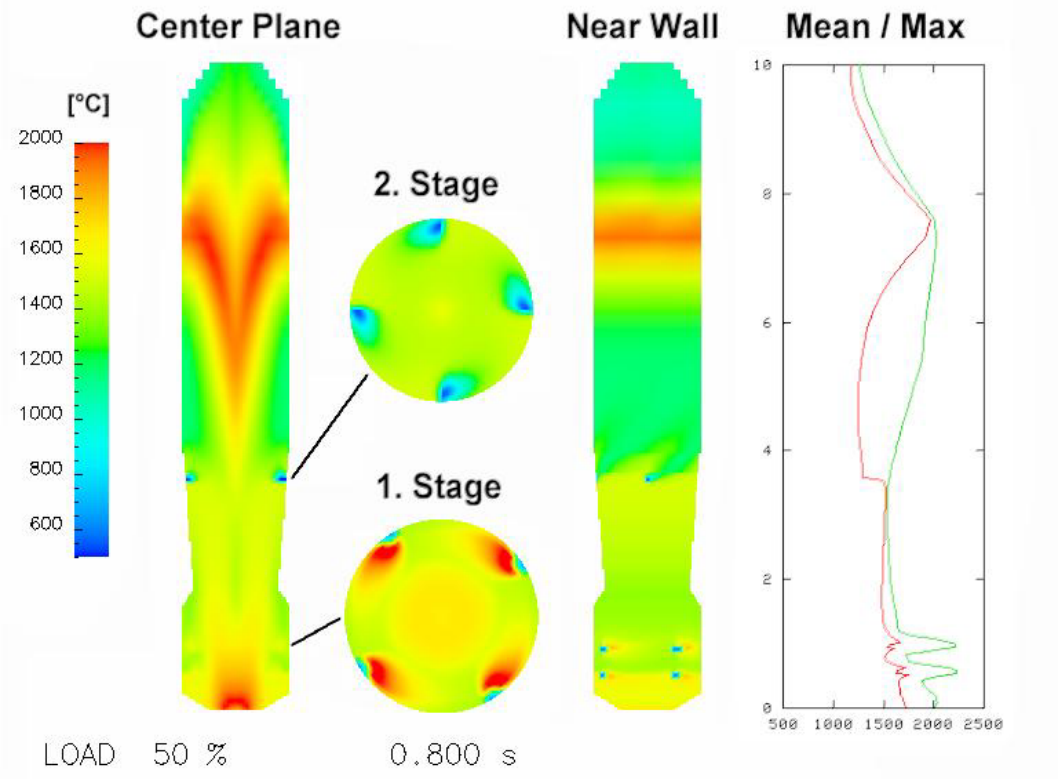

Figure 32: Computational results of inner, near wall, and mean temperature (t = 0.8 s)

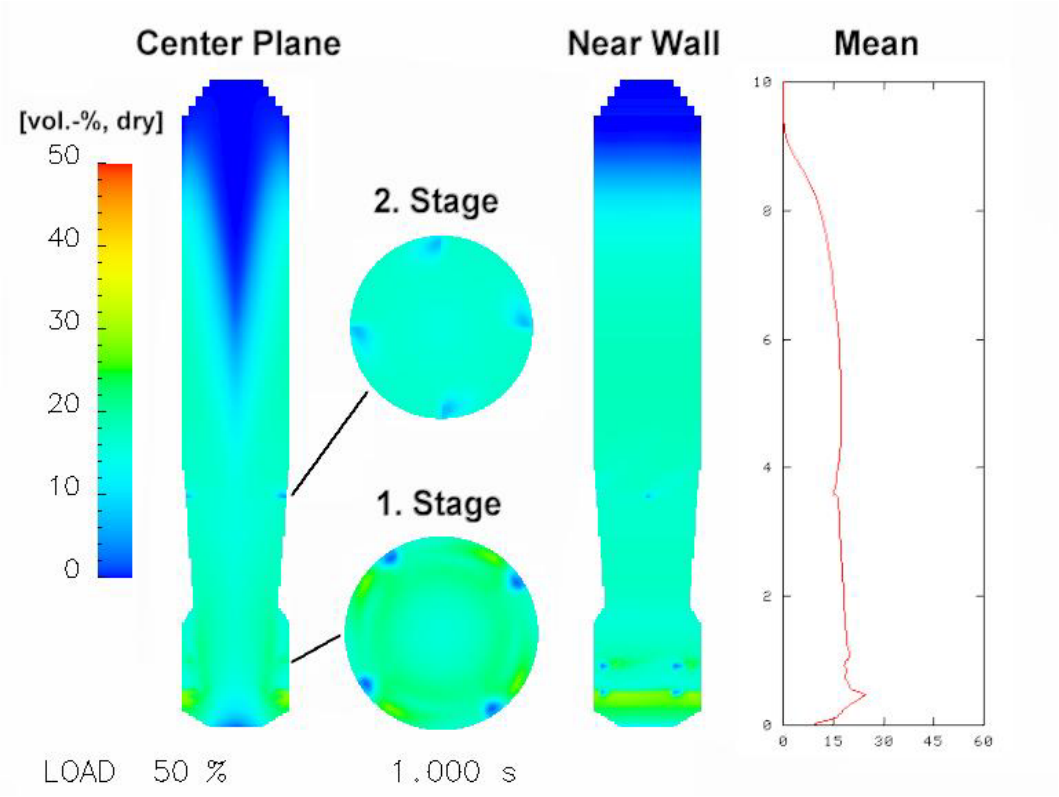

Figure 33: Computational results of inner, near wall, and mean CO-concentrations (t = 1.0 s)

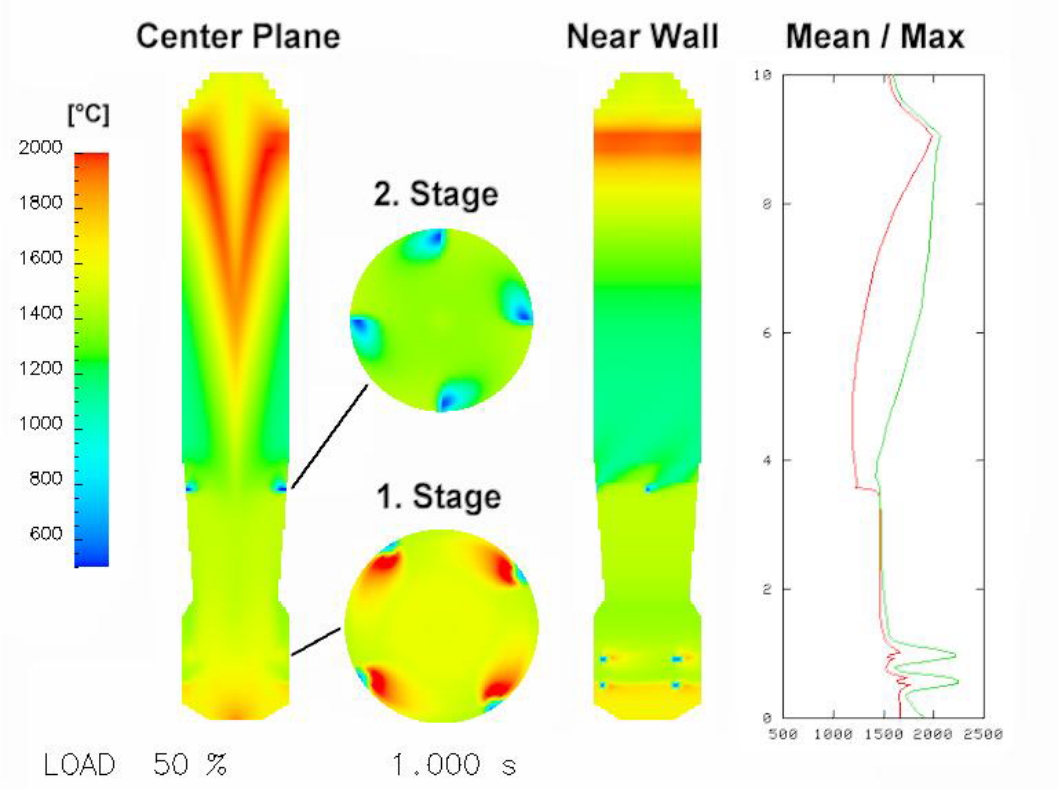

Figure 34: Computational results of inner, near wall, and mean temperature (t = 1.0 s)

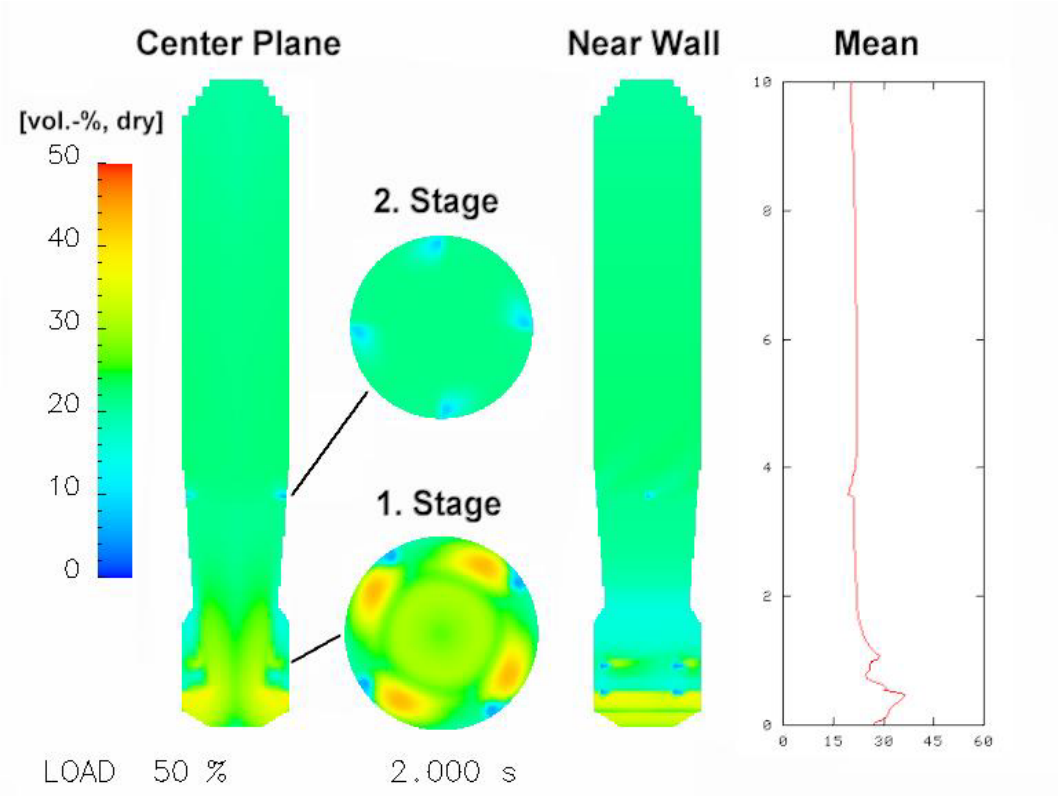

Figure 35: Computational results of inner, near wall, and mean CO-concentrations (t = 2.0 s)

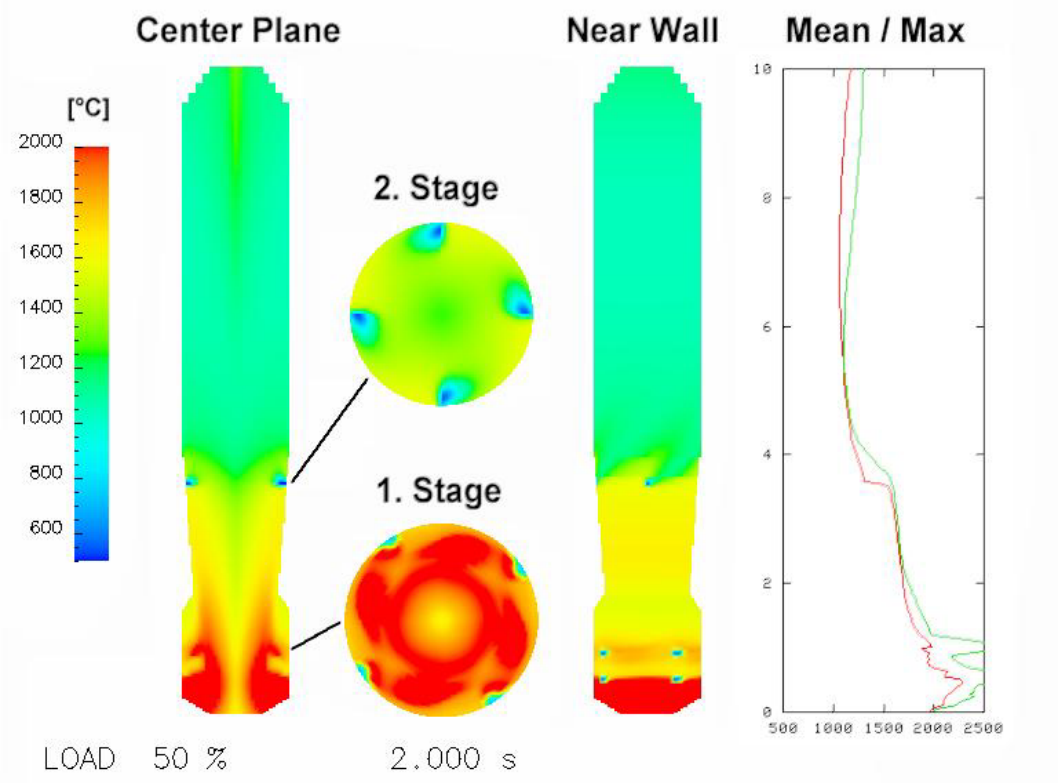

Figure 36: Computational results of inner, near wall, and mean temperature (t = 2.0 s)

Conclusions

During the last quarter good progress has been made on the development of an IGCC workbench. A Vision 21 workbench that contains a full complement of component models is available for use. Calculations for a full Vision 21 plant configuration have been performed for two types of entrained flow gasifiers. Good agreement with DOE computed values has been obtained for the Vision 21 configuration under "baseline" conditions. Transient, CFD simulations for the start-up of a gasifier have been performed using a standalone unsteady, gasifier CFD modeling tool executing on a supercomputer. A process model has been completed and implemented into the workbench that can simulate one and two stage gasifiers that use slurry or dry feed; the model is not limited to assuming complete burnout of the fuel in the first stage of the gasifier. A standalone, pre-processor module is under development that will compute global gasification rate parameters from standard fuel properties and intrinsic rate information. Work has started on developing standalone models for a membrane based water gas shift reactor and for "combustors" to oxidize the unburned fuel contained in the exhaust gas from a fuel cell. The IGCC workbench has been modified to use the VTK data visualization package that supports advanced visualization methods, including low-end Virtual Reality techniques. A whitepaper has been completed that describes the findings and recommendations from this project on the appropriate use of component architectures, model interface protocols and software frameworks for developing a Vision 21 plant simulator. A "live" demonstration of the Vision 21 workbench that highlighted the ease-of-use, functionality and plug-and-play features of the workbench was provided at a DOE sponsored coal utilization conference.

Plans for the next quarter include: implement into the workbench a membrane based water gas shift reactor model, fuel cell exhaust gas oxidizer models, an improved entrained flow gasifier model and an improved fuel cell model; perform plant simulations to explore and exercise the capabilities of the Vision 21 workbench and to evaluate the impact on predicted plant performance of using alternative gasifier operation and new/improved downstream equipment models; and implement into the workbench software from the Iowa State University (ISU) Virtual Reality Application Center that will provide compatibility with DOE-NETL and ISU immersive Virtual Reality facilities.

References

Bockelie, M.J., Swensen, D.A., Denison, M.K., Senior, C.L, Chen, Z., Linjewile,, T., Sarofim, A.F., and Risio, B., "A Computational Workbench Environment for Virtual Power Plant," Technical Progress Report #8 (July-September, 2002) for DE-FC26-00NT41047, October, 2002.

Bockelie, M.J., Swensen, D.A., Denison, M.K., Senior, C.L, Chen, Z., Linjewile,, T., Sarofim, A.F., and Risio, B., "A Computational Workbench Environment for Virtual Power Plant," Technical Progress Report #9 (October-December, 2002) for DE-FC26-00NT41047, January, 2003 (a).

Bockelie, M.J., Swensen, D.A., Denison, M.K., Maguire, M., Chen, Z., Linjewile,, T., Senior, C.L., Sarofim, A.F., "A Process Workbench for Virtual Simulation of Vision 21 Energyplex Systems," *Proceedings of the 28th International Technical Conference on Coal Utilization & Fuel Systems*, Clearwater, Florida, USA, March 10-13, 2003(b).

Bockelie, M.J., Sarofim, A.F., Denison, M.K., Swensen, D.A., Maguire, M., Weinstein, D., Davison de St. Germain, J., "Computational Workbench Environment for Virtual Power Plant Simulation," poster presented at the 28th International Technical Conference on Coal Utilization & Fuel Systems, Clearwater, Florida, USA, March 10-13, 2003(c).

Bockelie, M.J., Denison, M.K., Chen, Z., Linjewile, T., Senior, C.L., Sarofim, A.F., "Using Models To Evaluate Gasifier Performance," to be included in the *Proceedings of the 20th Annual International Pittsburgh Coal Conference,* Pittsburgh, PA, USA, Sept. 15-19, 2003 (d).

Bond, T. C., Noguchi, R.A., Chou, C-P., Mongia, R.K., Chen, J-Y and Dibble, R.W., "Catalytic combustion of natural gas over supported platinum: Flow reactor experiments and detailed numerical modeling." *American Society of Mechanical Engineers Technical Papers.* 96-GT-130, 1996.

Bracht, M., P.T. Alderliesten, R. Kloster, R. Pruschek, G. Haupt, E. Xue, J.R.H. Ross, M.K.Koukou, N. Papyannokos, "Water gas shift membrane reactor for CO_2 control in IGCC systems: techno-economic feasibility study," Energy Convers. Mgmt Vol. 38, Suppl., pp. S159-S164, 1997.

Chou, C-P., Chen, J-Y., Evans, G.H. and Winters, W.S., "Numerical Studies of Methane Catalytic Combustion Inside a Monolith Honeycomb Reactor Using Multi-Step Surface Reactions." *Combust. Sci. and Tech*., Vol 150 pp27-57, 2000.

Damle,A.S., T.P. Dorchak, "Recovery of carbon dioxide in advanced fossil energy conversion processes using a membrane reactor," DOE Contract No. DE-AC26-98FT40413.

Damle,A.S., S.K. Gangwal, V.K. Venkataraman, "A simple model for a water gas shift membrane reactor," Gas Sep. Purif. 8, p. 101. 1994.

Denison, M.K., Bockelie, M.J., Chen, Z., Senior, C.L., Linjewile, T., Sarofim, A.F., "CFD-Based Models of Entrained-Flow Coal Gasifiers with Emphasis on Slag Deposition and Flow," to be presented at the Colloquium on Black Liquor Combustion and Gasification, Park City Utah, USA, May 13-16, 2003.

Devarajan T.S, Peter N. Pintauro, "The water gash shift reaction assisted by a palladium membrane reactor," Ind. Eng. Chem. Res. 30, pp 585-589, 1991.

Edlund, D.J., "A catalytic membrane reactor for facilitating the water-gas shift reaction at high temperature," DOE Contract No. DE-FG03-91ER81229, in Coal-Fired Power Systems 94 – Advances in IGCC and PFBC Review Meeting, Morgantown, WV, July 21-23, 1994.

Fletcher TH;Kerstein AR;Pugmire R J; Solum MS; Grant DM Energy Fuels 1992, 6, 414-431.

Gavalas, G.R. *Combustion Science & Technology*, 24, pp.197-210, 1981.

Gemmen, R.S., "Oxidation of Low Calorific Value Gases—Applying Optimization Techniques to Combustor Design," U.S. DOE FETC, Presented at the 1998 IJPGC, Baltimore, MD, Aug 23-26, 1998.

Ghezel-Ayagh , H. and Maru, H. "Direct Fuel Cell/Turbine System for Ultra High efficiency Power Generation." *2002 Fuel Cell Seminar*, November 18-21, Palm Springs, California, pp.356-359. 2002

Kobayashi H; Howard JB; Sarofim AF 16th Symp. (Int'l.) on Combustion. The Combustion Institute, 1976.

Kolaczkowski, S.T., "Catalytic Stationary Gas Turbine Combustors: A Review of the Challenges Faced to Clear the Next Set of Hurdles." *Trans IchemE*, vol 73, Part A, 1995 pp168-190.

Ma, D., C. R.F. Lund, "Assessing High-Temperature Water-Gas Shift Membrane Reactors," Ind. Eng. Chem. Res. 42, pp711-717, 2003.

Marigliano, G., G. Barbieri, E. Drioli, "Effect of energy transport on a palladium-based membrane reactor for methane steam reforming process," Catalysis Today 67, pp. 85-99, 2001.

Muris S; Haynes BS, manuscript in preparation, 1999.

Smith, G.P., Golden, D.M., Frenklach, M., Moriarty, N.W., Eiteneer, B., Goldenberg, M., Bowman, C.T., Hanson, R.K., Song, S., Gardiner, W.C., Jr., Lissianski, V.V., and Qin, Z., `http://www.me.berkeley.edu/gri_mech/`

Smith, IW, Combustion and Flame 1971, 17, 421.

Sun, J. and Hurt, R.H., "Mechanisms of Extinction and Near-Extinction in Pulverized Solid Fuel Combustion," *Proceedings of the Combustion Institute, Vol. 28,* pp. 2205-2213, 2000.

Swensen, D.A., Denison, M.K., Maguire, M., Bockelie, M.J., Montgomery, C.J., Davison de St. Germain, J., "Computational Simulation Environments," poster presented at the Society of Industrial and Applied Mathematicians (SIAM) Computational Sciences and Engineering Conference 2003, San Diego, California, USA, February 10-14, 2003 (a).

Swensen, D.A., Yang, C., Maguire, M., Shino, D., Parker, S., Weinstein, D., Davison de St. Germain, J., "Model Interchangeability via Component Architectures for Vision 21 Simulation Environments," poster presented at the 28th International Technical Conference on Coal Utilization & Fuel Systems, to be held in Clearwater, Florida, USA, March 10-13, 2003(b).

Tucci, E.R. "Use Catalytic Combustion for LHV Gases." *Hydrocarbon Processing*, pp159-166, 1982.

Appendix

Component Software Issues for Vision 21 Plant Simulation and Engineering – Findings and Recommendations

Executive Summary

During the last two years there has been substantial effort invested by DOE and DOE contractors to better define the needs of Vision 21 simulations. The goal of these efforts has been to identify the appropriate software techniques and capabilities to embody within Vision 21 plant simulator systems to ensure these simulators can support the hierarchy of models and simulation techniques that will be used in near term and future Vision 21 plant simulations.

In this manuscript we summarize our findings and recommendations on the issues of component architectures and component interfaces that are relevant to Vision 21 plant engineering and simulation. These concepts relate to advanced software engineering techniques, originally developed for business applications, that have recently been adopted by the scientific computing community. The advent of the Vision 21 program has probably been the first instance of these software techniques being used in simulations for power generation applications. To keep our descriptions brief, we provide summaries, written in "layman terms", on component architectures (e.g., COM, CORBA, CCA), component interfaces (e.g., CAPE_Open) and software frameworks (e.g., ASPEN, SCIRun). We highlight only the key concepts that are relevant to Vision 21 simulation. As described below, direct comparisons between items at different levels of the software engineering hierarchy (e.g., CCA .vs. CAPE_Open) are not appropriate.

Our findings are based on research performed within our Vision 21 project, in conjunction with discussions with personnel involved with Vision 21 and with leading researchers in the fields of high performance computing and scientific computing.

Our findings lead to the following **recommendations**:

1. **Near term**: Vision 21 simulator frameworks should **support** both **COM** and **CORBA** component architecture versions of the **CAPE_Open** interface standard. We anticipate continued, extensive use of "process flow sheet" models within Vision 21 plant simulations and engineering. This component interface will allow use of process models developed for process flow sheet simulations from commercial and research sources.
2. **Long term**: an **improved component model interface should be developed** and deployed to support specific needs of the Vision 21 simulator. In particular, the inherent limitations on data transfer between components imposed by the CAPE_Open interface should be eliminated to allow utilization of more comprehensive modeling techniques. The enhanced component interface could be developed through judicious extensions to the CAPE_Open standard or by creating a new specification targeted for Vision 21.
3. **Frameworks:** We recommend **continued development of Vision 21 simulator framework(s)** that can support the hierarchy of models anticipated for future Vision 21 plant simulations. In the near term, commercially available frameworks (e.g., ASPEN) will continue to play an important role in Vision 21 simulation. However, it is unclear that there is sufficient motivation for commercially available frameworks to invest the funds needed to extend their simulation tools to have the flexibility and extensibility desired for advanced plant simulation.

Introduction

Over the course of the last decade, component architectures have revolutionized business software design and implementation. Based on the successes attained in the business software world, developers of scientific computing applications have, over the last several years, taken significant interest in this paradigm. The key features of component methods that make them so attractive for scientific computing are:

- interoperability of software (reuse)
- programming language independence and
- location transparency.

It is the goal of this document to educate the reader regarding component architecture technology being used to target scientific applications and provide recommendations on how this technology applies to Vision 21 plant simulations.

Background

As software engineering techniques evolved during the early 1990's, it was recognized that the current model for code reuse and application engineering was constrained at best. This original model relied on the use of static and dynamic libraries which contained code (both modular and/or objected-oriented) which could be directly linked to an application core.

One of the problems with this paradigm is that developers were highly constrained by the language used to generate the libraries. If an application developer was using a language different from that of the libraries, a significant amount of specialty, platform specific code needed to be generated to utilize the libraries. Also, this paradigm provided no inherent capabilities for platform independence or location transparency. Finally, code reuse was very limited due to the aforementioned language problems and also as a result of non-standard software interfaces (data structures, function parameters etc) used by functions and objects in the libraries.

How did these problems affect scientific and engineering applications? Most notably by limiting code reuse (interoperability), by causing programming language incompatibilities and by requiring extra development effort for any distributed parallelism (executing on remote computational resources).

Component Architecture Concepts

To address these shortcomings, component architectures and component programming models were developed. Component methods specifically target the problems of language independence, location transparency and interoperability of software. The component programming model is the end of a natural progression, starting from the monolithic application (the old paradigm), and moving toward applications built from increasingly more modularized pieces.

Historically, work on component architectures has been motivated by business-oriented computing. Application of component architectures to scientific and engineering applications is a relatively new endeavor (within last ~5 years).

Component architectures are a step beyond object-oriented programming, where software exists as components of functionality which interact through well defined interfaces. This is a bit of a fuzzy concept which requires some elaboration.

Example: Let's begin with an example of a relatively simple component which would have broad applications to scientific computing. Assume we want to create a "component" which will be capable of solving a linear system of the form Ax=b.

> To begin with, we would write a component interface in a special language called IDL (Interface Definition Language). This language, which is a function of the component architecture chosen, is specifically designed to create ***interfaces*** – not the equation solver software itself. The IDL written for this example would define language independent data structures for the matrices, methods (functions) for changing the solution techniques and for setting problem parameters. This is the first step in creating a component.
>
> After the IDL has been written, we use an IDL compiler to compile the IDL code. When we compile the IDL code, we must tell the compiler which programming language to use (C++, FORTRAN, Java, etc). The IDL compiler then creates a programming language specific implementation of our language-independent IDL. We can then take the code generated by the IDL compiler and write the actual implementation of the solver in the appropriate methods of the component.
>
> A developer wishing to use our component would obtain a copy of the IDL code from us and would then compile the code using their language of choice. The developer will now have access to language specific prototype information for the component, which they would then use to access the desired functionality.

One should note that the component developed in this example could be executed on any platform that has an implementation of the target component architecture. Also, the developer need not execute the component on the same computer as their application, which makes use of this component. The details of this location transparency are encapsulated in the specific component architecture being used.

To summarize, the following steps are required to construct and utilize a component in an application (see Figure A1):

- Choose the component architecture of interest (depends on platform, performance requirements, required data structures)
- Write the ***software interface*** to the component using the IDL belonging to the component architecture chosen in previous step
- Compile the IDL code using the IDL compiler

- Flush out the code generated by the IDL compiler with the details of component's implementation (i.e., code to solve Ax=b)
- An application requiring the component's functionality can now include client-side code generated by the IDL compiler and make calls to the component via the ***software interface***

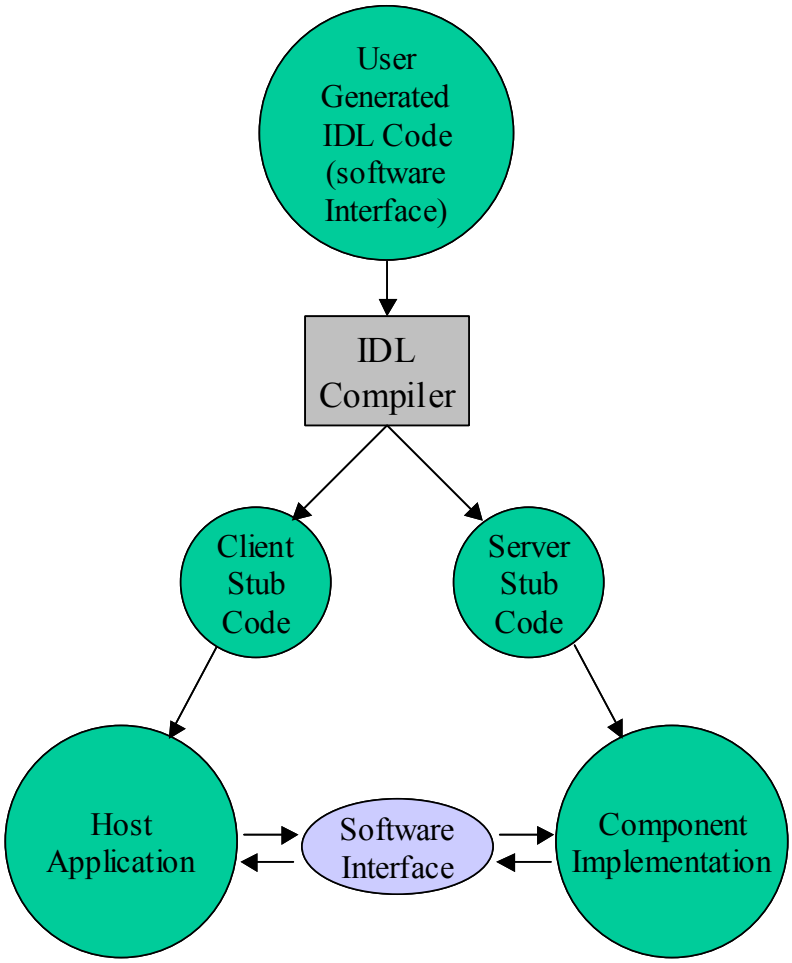

Figure A1. Component creation steps.

Standard Interfaces

While components have allowed us to solve most of the problems associated with language interoperability and location transparency, we haven't discussed the issue of ***standard interfaces***. This is a very important topic, especially when we are interested in code reuse and interoperability. ***There is tremendous motivation to make use of software components, created by other developers, in new software we are creating.*** One can imagine the power of being able to construct scientific applications as compositions of pre-existing functional components.

To make this a reality, we must define standard, domain specific ***interfaces*** which clearly define how components with different types of functionality interact with the outside world. Such

standard interfaces make possible a paradigm where a host software application (the ***framework***) can be used to instantiate and interconnect various components with well-defined interfaces to construct an application.

To date, the most significant set of standard interfaces for a domain-specific scientific application is CAPE-Open. CAPE (Component Architectures for Process Engineering) was created to address the needs of the chemical process modeling industry. The goal was to create interoperability and re-use of models developed for use in the large process simulation frameworks (Aspen Plus, Hysys, etc). CAPE is an excellent step in the direction of increased reuse and interoperability for the process simulation community. CAPE interfaces have been created for both COM and CORBA IDL's (see "Flavors of Component Architectures").

Although the CAPE interface specifications are very capable for process engineering problems, one must keep in mind that they were designed specifically for process engineering applications where simple single point scalar data (bulk temperature, pressure, species concentrations, flow rate, etc) is passed to and from components. This in no way detracts from the capabilities of CAPE for process engineering, but must be considered when higher order models and other functional entities must be included in a simulation framework composition.

In the high performance computing (HPC) community, numerous efforts are underway to generate standard interfaces for various problem domains such as solvers, mesh manipulation, visualization components, etc. Continued work in this area will lead to a new era in modular HPC applications.

Flavors of Component Architectures

What exactly is a component architecture? A given component architecture is the low-level software that provides all the capabilities that we have discussed in the previous sections. These include the IDL language and IDL compiler, the necessary libraries to perform network communications (where applicable), the "controller" software which receives and processes requests to instantiate components and numerous other low-level capabilities. There are three main component architectures which are of interest to scientific application developers.

COM/DCOM

COM/DCOM (Component Object Model/DistributedCOM) is the component architecture developed by Microsoft Corporation. It is by far the most widely used general purpose CA. Anyone who uses Microsoft Windows in any of its recent incarnations makes extensive use of COM without even knowing it. Windows uses COM for virtually everything, including their user interface and many core operating system elements. There exists a somewhat small but growing interest in applying COM to scientific applications.

CORBA

CORBA (Common Object Request Broker Architecture) is a widely used, business-oriented component architecture standard developed by the Object Management Group (OMG). The OMG is an open membership, not-for-profit consortium that produces and maintains computer

industry specifications for interoperable enterprise applications. Membership includes virtually every large company in the computer industry, and hundreds of smaller ones. While lacking in the high performance features of the CCA, the wide user base of CORBA and its mature implementations makes it a logical choice for small-to-medium sized computational models.

CCA

CCA (Common Component Architecture) is the newest component architecture and the only one that is targeted specifically to high performance scientific computing applications. The CCA effort is funded through the Center for Component Technology for Terascale Simulation Software (CCTTSS), which is dedicated to the development of a component-based software development model suitable for the needs of high-performance scientific simulation (CCA).

The Center is funded by the U. S. Dept. of Energy (DOE) as an Integrated Software Infrastructure Center (ISIC) under the Scientific Discovery through Advanced Computing (SciDAC) program and includes members from Argonne, Livermore, Los Alamos, Oak Ridge, Pacific Northwest, and Sandia National Laboratories, Indiana University and the University of Utah.

The CCA specification is still under development although numerous applications have been developed using the current specification. CCA was created to overcome the limitations of the business-oriented CA's (COM/CORBA) with regard to data passing, parallelism, memory management etc. CCA is seeing tremendous growth in the high performance computing community.

In addition to enhanced performance, CCA boasts some unique capabilities which further differentiate it from the traditional CA's. Of particular note is its rich IDL (SIDL – Scientific Interface Definition Language) which contains a wide array of data types and data structures needed in scientific computing. CCA's SIDL compiler is also the only IDL compiler that can generate FORTRAN 77 and FORTRAN 90 bindings making it particularly useful for legacy scientific application porting.

Although CCA is the clear winner in terms of targeting high performance scientific computing applications, it is still quite early in development. The available frameworks and associated tools are currently limited to Unix/Linux platforms and require significant expertise to configure and use. With the current significant interest in CCA and continued funding for its development, CCA is and will continue to be the CA of choice for HPC scientific applications.

It should be emphasized that CCA is targeted at HPC software. Specifically, CCA is intended to be used to componentize submodels of detailed computational models. When used in this manner, CCA is far superior to both COM and CORBA. This intra-model componentization is a more demanding application than that of providing a plug-and-play environment for connecting elements of a Vision21 plant together. Although CCA could certainly be used for the plant coupling, the additional complexity of CCA is really overkill for the application.

Overall Structure of Component-based Software with Standard Interfaces

Now that we have discussed the various entities which constitute a component-based application, let's see how the pieces fit together. Figure A2 provides an overview of the software structure. As a result of using standard interfaces, we are able to utilize a host application framework (center) that "speaks the language" of the standardized component interfaces. This allows us to plug-and-play compliant components within the framework with no coding required.

The standard interfaces shown in Figure A2 are represented by circles that lie between the framework and the underlying components. Interfaces shown in the figure include CAPE-Open and V21, with COM, CORBA and CCA underlying CA's. Note that the V21 software interface does not currently exist (see "Recommendations for Application of CA's to Vision21 Simulation Environments").

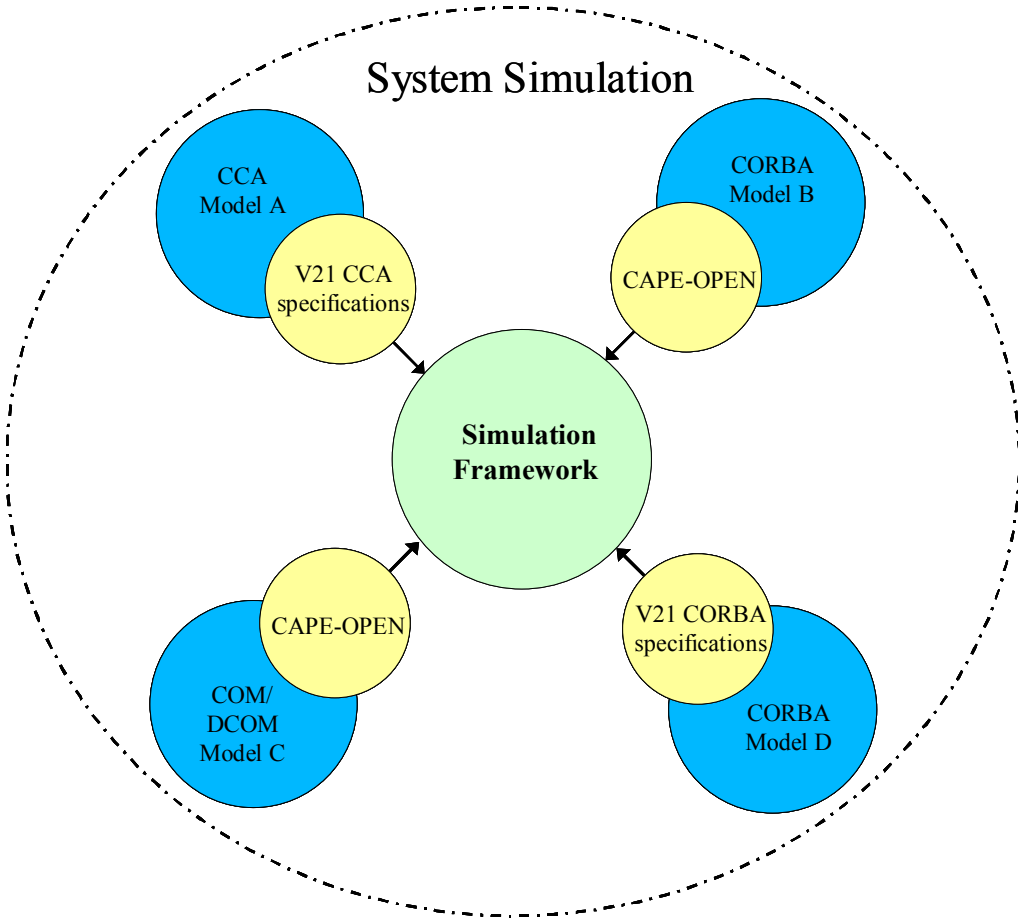

Figure A2. Use of standard component interfaces

Recommendations for Application of CA's to Vision21 Simulation Environments

Clearly, the advantages of CA's and standard interfaces would be very beneficial to Vision21 simulators. By supporting CA's, the Vision21 simulation projects will benefit by gaining access to software components being developed by numerous groups, unrelated to the Vision21 program, as well as software being developed internal to the Vision21 project. Also, software developed for the Vision21 program using these principals will be significantly more extensible and usable as the program continues to evolve and possibly mutate into other efforts.

Roadmap

To achieve these capabilities for Vision21 simulators, we suggest a phased approach to transitioning to CA and standard interfaces. First, we must define which CA's will be targeted and then select or create appropriate standard interfaces. Second, we must choose frameworks which are capable of utilizing these types of components.

CA and Standard Interfaces – As a first step, we suggest supporting both the COM and CORBA versions of the CAPE-Open interface. As noted earlier, CAPE is a very viable choice for process engineering models with limited data transfer needs. As a second step, we to address the needs of more comprehensive models in the simulation, we suggest creating an interface specification, specific to the Vision21 program ("V21" in Figure A2). The target CA's for this specification would be COM, CORBA and CCA. Note that the initial "V21" interface specification would be limited to defining how Vision21 plant component models communicate and interact with one another. Future enhancements to "V21" would likely include interface capabilities for lower level detailed modeling which would mandate implementing this portion of the interface using CCA SIDL.

By using the appropriate framework, both the CAPE and V21 interface specifications could be used. Using this approach, we achieve the "best of both worlds" by leveraging all the work done by the CAPE/processing engineering community, while using the V21 interface specification for more complex development tasks.

COM and CORBA CA's, with appropriate interface specifications, will meet the short term needs of the Vision21. However, long term, we believe CCA will be an important element of future Vision21 simulations. There is a significant amount of sophisticated modeling software currently being developed as CCA components. It would be beneficial to the Vision21 program to leverage this future source of high performance computing components. As a result of this consideration, we recommend that the framework chosen for use with Vision 21 simulators should be capable of working with CCA components.

Frameworks – For doing more simplistic modeling, Aspen Plus is a viable framework because it supports CAPE-Open components and is currently capable of using Fluent (via CAPE) to perform detailed simulations which return point (bulk) data. The problem with using Aspen Plus as a framework for the future of Vision21 stems from the limitation that only single point

information is passed between models. This limitation exists not only with the CAPE-Open interface, but also with Aspen itself. Being a commercial product, it is highly unlikely that Aspen would be modified to support other CA standards (V21) that would have very limited commercial application.

To support the hierarchy of models required for Vision21 (ranging from very simple response surface models to fully detailed CFD models), we need a framework which can support not only the simple models implemented with CAPE, but also the models developed using the more sophisticated interface developed for Vision21. This framework could be created by modifying an existing framework (such as SCIRun) or by creating a new framework specifically targeting Vision21 simulations. These decisions will depend in large part on who the end users of the simulation environments will be (and their level of expertise) and also the computer platforms they will be using for the simulations (Windows, Linux, Unix, etc).